LM-01K103
October 22, 2001

Measurement and Calculation of Electrochemical Potentials in Hydrogenated High Temperature Water, including an Evaluation of the Yttria-Stabilized Zirconia/Iron-Iron Oxide (Fe/Fe_3O_4) Probe as a Reference Electrode

Steven A. Attanasio, David S. Morton, Mark A. Ando

NOTICE

Measurement and Calculation of Electrochemical Potentials in Hydrogenated High Temperature Water, including an Evaluation of the Yttria-Stabilized Zirconia/Iron-Iron Oxide (Fe/Fe_3O_4) Probe as a Reference Electrode

Steven A. Attanasio, David S. Morton and Mark A. Ando
Lockheed Martin Corporation
Schenectady, NY 12301

ABSTRACT

The importance of knowing the electrochemical corrosion potential (ECP, also referred to as E_{corr}) of nickel-base alloys in hydrogenated water is related to the need to understand the effects of dissolved (*i.e.*, aqueous) hydrogen concentration ($[H_2]$) on primary water stress corrosion cracking (PWSCC). Also, the use of a reference electrode (RE) can improve test quality by heightening the ability to detect instances of out-of-specification or unexpected chemistry. Three methods are used to measure and calculate the ECP of nickel-based alloys in hydrogenated water containing ~ 1 to 150 scc/kg H_2 (0.1 to 13.6 ppm H_2) at 260 to 360°C. The three methods are referred to as the specimen/component method, the platinum (Pt) method, and the yttria-stabilized zirconia/iron-iron oxide (YSZ/Fe-Fe_3O_4) RE method. The specimen/component method relies upon the assumption that the specimen or component behaves as a hydrogen electrode, and its E_{corr} is calculated using the Nernst equation. The present work shows that this method is valid for aqueous H_2 levels ≥ ~ 5 to 10 scc/kg H_2. The Pt method uses a voltage measurement between the specimen or component and a Pt electrode, with the Pt assumed to behave as a hydrogen electrode; this method is valid as long as the aqueous H_2 level is known. The YSZ/Fe-Fe_3O_4 method, which represents a relatively new approach for measuring E_{corr} in this environment, can be used even if the aqueous H_2 level is unknown. The electrochemical performance of the YSZ/Fe-Fe_3O_4 probe supports its viability as a RE for use in high temperature hydrogenated water. Recent design modifications incorporating a teflon sealant have improved the durability of this RE (however, some of the REs do still fail prematurely due to water in-leakage). The Pt method is judged to represent the best overall approach, though there are cases where the other methods are superior. For example, the specimen/component method provides the simplest approach for calculating the E_{corr} of plant components, and the YSZ/Fe-Fe_3O_4 RE method provides the best approach if the H_2 level is unknown, or in off-nominal chemistry conditions. The present paper describes the use of these methods to determine the ECP of a specimen or component versus the ECP of the nickel/nickel oxide (Ni/NiO) phase transition, which is important since prior work has shown that this parameter ($ECP - ECP_{Ni/NiO}$) can be used to assess aqueous H_2 effects on PWSCC.

BACKGROUND

The importance of being able to measure and/or calculate ECPs is related to the need to understand and predict the effects of aqueous H_2 level on PWSCC. It has been clearly shown that aqueous H_2 influences PWSCC [1-5]. However, evidence has been presented [3, 4] that ECP is a more fundamental measure of environmental effects on PWSCC. According to Cassagne [6], "the role of hydrogen is to fix the potential and consequently to control the oxide composition". In fact, aqueous H_2 effects are more readily understood if the data are correlated using the parameter 'ECP *vs.* the Ni/NiO equilibrium' (*i.e.*, $ECP - ECP_{Ni/NiO}$ or, alternatively, $ECP_{Ni/NiO} - ECP$) [3, 4]. As shown in Figure 1, the maxima in SCC growth rate for three nickel-based alloys resides near the ECP of the measured Ni/NiO transition when data from multiple temperatures are plotted using this parameter [4, 7, 8]. The Ni/NiO phase transition used to construct Figure 1 is based on contact electric

resistance (CER) and corrosion coupon measurements [7]. Previous work [9] has shown that Pt behaves as a hydrogen electrode in high temperature hydrogenated water, and that Ni-based alloys often exhibit similar behavior. This observation is useful since potentials can be calculated and referenced to the standard hydrogen electrode (SHE) scale by using the Nernst equation to calculate the E_{corr} of the hydrogen exchange reaction at the temperature, pH and H_2 level of interest. Electrodes based on the YSZ system (*e.g.*, Cu/Cu_2O, Hg/HgO, Ag/Ag_2O, Fe/Fe_3O_4) have been used as pH electrodes in previous studies [10], and acceptable performance relative to Pt (acting as a hydrogen electrode) was demonstrated at temperatures from 175 to 275°C [11]. It was pointed out by Niedrach [12] that if the pH of a given system is essentially constant and readily calculable, a YSZ-based electrode can also serve as a RE. In fact, YSZ-based electrodes have been used successfully as REs in boiling water reactor (BWR) environments at 288°C [13]. However, a detailed evaluation has not been performed for PWSCC environments, in which testing is typically conducted at higher temperatures and at much higher aqueous H_2 concentrations compared to either normal water chemistry (NWC) or hydrogen water chemistry (HWC) BWR environments. (*e.g.*, ~ HWC tests are typically conducted at ~ 0.15 ppm H_2 [14], which corresponds to ~ 1.7 scc/kg H_2). The YSZ/Fe-Fe_3O_4 RE has several key benefits: (i) it does not introduce contamination (*e.g.*, chlorides) into the environment, (ii) it can be operated without placing Teflon™ in the hot water (and thus can function at > 288°C), and (iii) its potential can be referenced to the SHE scale.

EXPERIMENTAL

Testing was conducted in deaerated water buffered to a high temperature pH of ~ 6.5 to 6.75. The desired H_2 concentrations were obtained by varying the feed tank H_2 overpressure according to Henry's law. The room temperature H_2 calculations were conducted using a Henry's law coefficient [15] of 0.85 psia/(scc/kg). Mixed gas of 4 or 14.7% hydrogen with the balance being argon was used to obtain aqueous H_2 levels less than 20 scc/kg H_2. ECP measurements were made using voltmeters with input impedance ≥ 10 GΩ. Testing was performed in recirculating autoclaves which have been described previously [16]. Additional details regarding ECP measurement hardware (*e.g.*, the YSZ/Fe-Fe_3O_4 RE) are discussed later in this paper.

The ECP data were supplemented in some cases by using a silver/palladium (Ag/Pd) tube to measure autoclave H_2 pressure at 260°C. This device has been used by others, mainly at high temperatures (*e.g.*, 360°C), as discussed by Scott [3]. The measurements were performed using a 75% Pd-25% Ag tube having 0.127 mm wall thickness, 4.7 mm outside diameter and 63.5 mm length; the tube also has an internal spine to support high external pressure. The Ag/Pd tube is brazed to a stainless steel (SS) cap on one end and to a SS tube on the other end, with the SS tube connected to a vacuum pump and a pressure transducer. The measurement is conducted by pumping down the inside of the tube and then valving the pump out of the circuit so that the pressure transducer registers the buildup of hydrogen gas within the tube. The vacuum formed by the pump creates a driving force for hydrogen in the autoclave to diffuse through and build up inside the Ag/Pd tube. The pressure in the tube builds up to a steady-state pressure, which is equal to the hydrogen partial pressure in the autoclave.

RESULTS

Details are provided in this section for the three methods used to measure and/or calculate E_{corr}. Only methods for which E_{corr} can be referenced to the SHE scale are discussed, since ECP measurements can only be quantitative in nature if the measurements are referenced to a standard scale.

Method (1): Specimen/Component Calculational Method: This method requires that the aqueous H_2 level, temperature, Henry's law coefficient and the pH at the temperature of interest be known. The specimen is assumed to act essentially as a hydrogen electrode (Figure 2), and thermodynamic data for the hydrogen exchange reaction are used to calculate the potential of the specimen or component. Data are plotted in Figure 3 to assess the ability of nickel and several types of nickel-based alloys (Alloy X-750 in the HTH and AH heat treatments and Alloy 600) to act as hydrogen electrodes. In Figure 3, it is shown that for nickel and the nickel-based alloy specimens, the steady-state electrochemical corrosion potential of the specimen is very similar to that of platinum (*i.e.*, within 0 to 6 mV, which is a minor difference) for aqueous H_2 levels $\geq$ ~ 5 to 10 scc/kg. Since platinum is known to act as a hydrogen electrode in this environment (based on prior work [9], and supported by data generated in the present study), Figure 3 implies that the E_{corr} of nickel or a nickel-based alloy can be readily calculated using available thermodynamic data for the hydrogen exchange reaction, provided that the aqueous hydrogen level is known *and* the concentration is $\geq$ ~ 5 to 10 scc/kg H_2. [1]

The reason why Ni-based alloys begin to deviate from hydrogen electrode behavior below ~ 5 to 10 scc/kg H_2 (Figure 3) while Pt continues to behave as a hydrogen electrode in this regime is related to the fact that a competing reaction (*i.e.*, metal oxidation) is present on the Ni-based alloys but not on Pt (Figure 4 (a)). For Ni-based alloys, at relatively high aqueous H_2 levels the rate of H_2 oxidation is much greater than the rate of metal corrosion, and thus the hydrogen oxidation reaction dominates the anodic kinetics, resulting in an E_{corr} that is only negligibly different from that of a hydrogen electrode (Figure 4(b)). However, since the rate of the H_2 oxidation reaction is monotonically related to the aqueous H_2 level, a point is eventually reached as the aqueous hydrogen level is lowered at which metal corrosion begins to influence the total anodic current, and thus affect the ECP (Figure 4(c)).

Procedure: The calculations utilize the Nernst Equation for the reaction $2\,H^+ + 2\,e^- \Leftrightarrow H_2$:

$$E^{SHE}_{hydrogen\ electrode} = E^{o}_{hydrogen\ electrode} - \frac{RT}{nF}\ln\frac{f_{H_2}}{a_{H^+}^{\,2}} \quad [Volts] \qquad [1]$$

- $E^{SHE}_{hydrogen\ electrode}$ is the electrochemical potential of the hydrogen exchange reaction *vs.* SHE (volts)
- $E^{o}_{hydrogen\ electrode}$ is the standard potential at unit fugacity and activity (volts) ($E^{\circ} = 0$ in equation [1])
- R is the universal gas constant (8.314 J/mol·K)
- T is temperature in Kelvin, K
- n is the number of electrons transferred in equivalents/mole (n = 2 in equation [1])
- F is Faraday's constant (96,500 coulombs/equivalent)
- f_{H_2} is the fugacity of H_2 (atmospheres), where $f_{H_2} = [H_2]\cdot H$
  - $[H_2]$ is the aqueous hydrogen concentration and H is the Henry's law coefficient
- a_{H^+} is the activity of hydrogen ions (where $a_{H^+} = [H^+] = 10^{-pH}$; $\ln a_{H^+} = -2.303\cdot pH$)

Equation [1] can be simplified to:

$$E^{SHE}_{hydrogen\ electrode} = -4.3x10^{-5}\cdot T\left(\ln([H_2]\cdot H) + 4.6\cdot pH\right) \quad [Volts] \qquad [2]$$

Table 1 provides the necessary input data for calculating E_{corr} via the specimen/component method.

[1] Figure 3 suggests that nickel may behave as a hydrogen electrode at lower coolant hydrogen values than Ni-based alloys.

Table 1. Data Needed for Hydrogen Electrode Calculations

Temperature (°C)	Temperature (K)	Henry's Law coefficient, H (atm/(scc/kg))	Test pressure[†] (psig)	Calculated pH (at temperature)
260	533	1.50×10^{-2}	1800	6.70
288	561	1.06×10^{-2}	1500	6.62
316	589	7.19×10^{-3}	3000	6.52
338	611	5.08×10^{-3}	3000	6.57
360	633	3.47×10^{-3}	3200	6.75

[†] The 288°C testing was performed at a lower pressure than the 260°C testing because it was performed more recently; test pressures were reduced to increase the likelihood of survivability of linear variable differential transformers (LVDTs) and YSZ/iron-iron oxide reference electrodes.

Henry's Law coefficients: The Henry's Law coefficients (Table 1) are taken from [15]. Unpublished hydrogen permeation data indicate that the existing Henry's Law correlation, on which these data are based, may be slightly in error; the uncertainty introduced by this issue is on the order of ~ 10 mV.

pH: The pH values were calculated using a high temperature thermodynamic code. Key parameters in the pH calculations are the concentration of pH additive and pressure used in the calculation, plus the presence/absence of a density correction. It is noted that when ECPs are measured *vs.* the YSZ/Fe-Fe_3O_4 RE or calculated versus the Ni/NiO equilibrium [4, 8], the pH term 'drops out' since the hydrogen electrode potential, the Fe/Fe_3O_4 equilibrium, and the Ni/NiO equilibrium all have the same pH dependence (*i.e.*, the same slope on a Pourbaix diagram).

Sample Calculation: For the Alloy 600 specimen tested at 120 scc/kg and 338°C (see Figure 3), the hydrogen fugacity is calculated as 0.61 atmospheres using the Henry's law coefficient in Table 1. Using equation [2] and Table 1, the ECP for the hydrogen electrode is calculated as: $E^{SHE}_{hydrogen\ electrode}$ = – 0.781 V_{SHE}; note that this value is consistent with our previously published data [4].

Benefits and Drawbacks: Method (1) is cost-effective, simple, and can be applied in situations where no RE data are available (*e.g.*, plant components or 'historical' autoclave test specimens). Method (1) is generally not useful in off-nominal environments (*e.g.*, in the presence of an oxidizer, which may cause the specimen ECP to deviate from hydrogen electrode behavior). Also, this method cannot improve test quality control by detecting inadvertant chemistry changes during a test.

Method (2): Platinum Electrode Method: Calculations are performed to determine the potential of a hydrogen electrode at the specified temperature and aqueous H_2 level using the Nernst equation. Then, the measured steady-state voltage difference between the specimen and the Pt electrode is added to the calculated Pt potential to calculate the specimen potential on the SHE scale:

$$E^{SHE}_{specimen} = E^{SHE}_{hydrogen\ electrode} + \left(E_{specimen} - E_{platinum}\right) \qquad [3]$$

It is important to electrically isolate the specimen and Pt electrode from all other metals when using methods (1) or (2) (particularly from metals such as zircaloy which do not behave as hydrogen electrodes), using ceramic, teflon (if ≤ 288°C) or thermally-oxidized zirconia [17].

At H_2 levels ≥ ~ 5 to 10 scc/kg, the difference between Methods (1) and (2) is negligible. However, if one considers the Alloy X-750 AH data point in Figure 3 at 0.7 scc/kg H_2 and 338°C, where the measured potential between Alloy X-750 AH and Pt is – 47 mV, the calculated Pt potential (*i.e.*, hydrogen electrode potential) is – 0.646 V_{SHE}, while the calculated specimen potential is – 0.693

V_{SHE}. A 47 mV difference may represent an appreciable error, and this example shows why Method (2) is the more accurate and preferred method at H_2 levels below ~ 5 to 10 scc/kg.

Evaluation of Pt as a Hydrogen Electrode: Figure 5 shows the E_{corr} of Pt versus Fe/Fe_3O_4 as a function of aqueous H_2 level at 316°C. The data follow the trend for the theoretical hydrogen electrode quite closely, with an offset of ~ 15 to 20 mV. Agreement within ± 10 mV has been termed 'excellent' for potentials measured using a high temperature RE [18]. The 15 to 20 mV offset is believed to be due to uncertainties in the thermodynamic values for the Fe/Fe_3O_4 equilibrium used to calculate the theoretical hydrogen electrode line. The offset in Figure 5 indicates that there is a systematic bias in either: (a) the ECP measurements or (b) the thermodynamic properties used to calculate the theoretical hydrogen potential. It is judged that (b) is much more likely, since the ECP measurements versus the YSZ/Fe-Fe_3O_4 electrode are relatively straightforward and are not subjected to any evident bias (it is shown later in this paper that the impedance of the YSZ/Fe-Fe_3O_4 probe does not introduce a bias to the measurements).[2] As shown in Figures 6 to 9 and in Tables 4, 5, 7 and 8, similar data to those in Figure 5 and Table 6 (316°C) have been obtained at 260, 288, 338 and 360°C.

Figure 10 shows a semi-logarithmic plot of the E_{corr} of Pt versus Fe/Fe_3O_4 as a function of the logarithm of aqueous H_2 level from 260 to 360°C. The evident linearity in the E vs. log $[H_2]$ data for each temperature indicates that the RE is behaving in a Nernstian manner. In fact, linearity is evident for more than two orders of magnitude in aqueous H_2 concentration at 338 and 360°C. The Nernst equation predicts that a larger negative slope for the E vs. log $[H_2]$ data should be observed as the temperature increases (Equation [2]). Figure 10 shows that the slopes at 260, 288, 316, 338 and 360°C are – 0.041, – 0.044, – 0.050, – 0.052 and – 0.059, respectively; this trend is consistent with theoretical expectations. Further, a quantitative comparison can be made between the slopes of the E vs. log $[H_2]$ data and the theoretical slopes derived from the Nernst equation. The theoretical slope is equal to the coefficient in equation [2] (*i.e.*, $-4.3\times10^{-5}\cdot T$), multiplied by 2.303 to account for the conversion between natural and base-ten logarithms. Figure 10 shows that the agreement with theory is reasonable, with errors of 23, 21, 14, 16, and 6% at 260, 288, 316, 338 and 360°C, respectively.

Method (3): YSZ/Iron-Iron oxide RE Method: This method requires only that the temperature and the pH be known, since the Fe/Fe_3O_4 equilibrium does not depend on the aqueous H_2 level. The measured potential is converted to the SHE scale using thermodynamic data for iron and iron oxide. A schematic diagram of the YSZ/Fe-Fe_3O_4 electrode is shown in Figure 11. The iron/iron oxide electrode is built by mixing Fe and Fe_3O_4 powder[3] and placing the mixture into a closed-end ceramic (YSZ) tube which is then immersed in the autoclave.[4] An equilibrium develops between the Fe and Fe_3O_4 (*i.e.*, $Fe_3O_4 + 8\ H^+ + 8\ e^- \Leftrightarrow 3\ Fe + 4\ H_2O$) which produces a constant potential on an iron or stainless steel wire immersed in the powder, at a given pH and temperature [12]. This concept can be

[2] Further, it is not uncommon for there to be some inaccuracies in high temperature thermodynamic metal/metal oxide calculations. For example, the theoretical Ni/NiO equilibrium calculated using thermodynamic data has been shown to be somewhat different than the experimentally measured Ni/NiO phase transition [7].

[3] General Electric has used the YSZ-based RE primarily in the Cu/Cu_2O form. In the present work, Cu/Cu_2O was not used due to concern that the autoclave would be contaminated with copper if the ceramic tube were to fracture near its tip.

[4] The ceramic tube provides a sheath for the Fe + Fe_3O_4 powder which prevents the mixture from becoming wet. It also serves as an oxygen ion conductor, which allows an equilibrium to develop between Fe, Fe_3O_4, H_2O and H^+. At the inner surface of the tube, the following equilibrium is established: $Fe_3O_4 + 4\ V_o^{\cdot\cdot} + 8\ e^- \Leftrightarrow 3\ Fe + 4\ O_o$ ($V_o^{\cdot\cdot}$ represents oxygen ion vacancies in the ceramic and O_o represents oxygen ions in the ceramic). The equilibrium at the outer tube surface is: $8\ H^+ + 4\ O_o \Leftrightarrow 4\ H_2O + 4\ V_o^{\cdot\cdot}$, yielding a net reaction of: $Fe_3O_4 + 8\ H^+ + 8\ e^- \Leftrightarrow 3\ Fe + 4\ H_2O$ (these reactions are based on those described for the YSZ/Hg-HgO electrode in [9]).

visualized in terms of the Fe Pourbaix diagram in Figure 2. The diagonal line labeled '13' corresponds to the equilibrium between Fe and Fe_3O_4. If the pH of the environment is essentially constant and reasonably well-known (as is the case for high temperature hydrogenated water), the Fe/Fe_3O_4 reaction exhibits a unique (and calculable) electrode potential on the SHE scale.

Procedure: Calculations are performed using the thermodynamics for the iron/magnetite reaction:

$$Fe_3O_4 + 8\,H^+ + 8\,e^- \Leftrightarrow 3\,Fe + 4\,H_2O \qquad [4]$$

The Nernst Equation for this reaction is written as:

$$E^{SHE}_{iron/iron\,oxide} = E^{o}_{iron/iron\,oxide} - \frac{RT}{nF}\ln\frac{a_{Fe}^{3}\cdot a_{H_2O}^{4}}{a_{Fe_3O_4}\cdot a_{H^+}^{8}} \quad [Volts] \qquad [5]$$

- $E^{SHE}_{iron/iron\,oxide}$ is the electrochemical potential of the iron/iron oxide reaction vs. SHE (volts)
- $E^{o}_{iron/iron\,oxide}$ is the standard potential of the reaction at unit fugacity and activity (volts)
- R, T, n, and F have been previously defined (note that $n = 8$ for reaction [4]).
- a_{Fe}, $a_{Fe_3O_4}$ *and* a_{H_2O} are the activity of iron, magnetite, and water [all are assumed = 1]
  - $a_{Fe} \cong a_{Fe_3O_4} \cong 1$ since these are pure solid species; $a_{H_2O} \cong 1$ since the environment is dilute

Using this information, equation [5] can be simplified to:

$$E^{SHE}_{iron/iron\,oxide} = E^{o}_{iron/iron\,oxide} - \frac{2.303RT}{F}\cdot pH \quad [Volts] \qquad [6]$$

Using thermodynamic quantities derived from magnetite testing by Ziemniak [19]:

$$E^{o}_{iron/iron\,oxide} = 0.073 - 1.38\times10^{-3}\cdot T + 1.47\times10^{-4}(T\cdot\ln T) \quad [Volts] \qquad [7]$$

Table 2 shows $E^{o}_{iron/iron\,oxide}$ values, pH values, and $E^{SHE}_{iron/iron\,oxide}$ values as a function of temperature.

Table 2. Iron/Iron Oxide Potentials as a function of temperature

Temperature (°C)	Temperature (K)	$E^{o}_{iron/iron\,oxide}$ (V)	Calculated pH† (at temperature)	$E^{SHE}_{iron/iron\,oxide}$ (V)
260	533	-0.171	6.70	-0.879
288	561	-0.179	6.62	-0.916
316	589	-0.187	6.52	-0.949
338	611	-0.194	6.57	-0.990
360	633	-0.200	6.75	-1.048

† The pH calculations were performed using the test pressures shown in Table 1. The pH and $E^{SHE}_{iron/iron\,oxide}$ values are similar, but not identical, to the values used previously [4] (a previous pH code was used in that work).

Equation [6] and Table 2 can be used to convert the measured specimen potential vs. Fe/Fe_3O_4 to SHE:

$$E^{SHE}_{specimen} = E^{SHE}_{iron/iron\ oxide} + (E_{specimen} - E_{iron/iron\ oxide})\ [Volts] \qquad [8]$$

Sample Calculation: Figure 5 (a) and Table 6 show that $E_{specimen} - E_{iron/iron\ oxide}$ for Alloy 600 at 120 scc/kg H_2 and 316°C is 0.177 V. According to Table 2, the $E^{SHE}_{iron/iron\ oxide}$ value at 316°C is – 0.949 V. Thus, the value of $E^{SHE}_{specimen}$ is – 0.772 V, as shown in Figure 5 (b) and Table 6.

Evaluation of Fe/Fe_3O_4 as a RE in High Temperature Hydrogenated Water:

Reasonableness check: According to Figure 2, the difference between the Fe/Fe_3O_4 equilibrium line and the standard hydrogen line (which corresponds to a fugacity of 1 atmosphere) is on the order of ~ 150 to 200 mV at 250°C. The best available comparison in the present study is at 260°C and 67 scc/kg H_2 (which corresponds to ~ 1 atmosphere according to the Henry's law coefficient in Table 1); however, there are no available Pt *vs.* YSZ/Fe-Fe_3O_4 data at this condition (Figure 6 (a)). It can be stated, though, that the Pt E_{corr} data are consistently located ~ 15 to 20 mV active to the theoretical hydrogen electrode line (*e.g.*, see Figure 5 (a)). Since the theoretical hydrogen electrode potential *vs.* the YSZ/Fe-Fe_3O_4 electrode at 260°C and 67 scc/kg H_2 is ~ 173 mV (Figure 6 (a)), it is expected that the potential of Pt *vs.* the YSZ/Fe-Fe_3O_4 electrode at 260°C and 67 scc/kg H_2 would be on the order of ~ 153 to 158 mV. Thus, the potentials measured in this study appear to be consistent with the values expected from the Pourbaix diagram.[5]

Evaluation versus a hydrogen electrode: Earlier in this paper, several different types of data were used to show that Pt appeared to behave as a hydrogen electrode in the present testing. Since all of the diagnostics used to prove this point rely upon data measured versus the YSZ/Fe-Fe_3O_4 electrode, the consistency of the measured platinum data with expected hydrogen electrode behavior implies that the YSZ/Fe-Fe_3O_4 electrode is truly functioning as a useful RE in this environment.

Reproducibility: Measurements versus the YSZ/Fe-Fe_3O_4 probe exhibit good reproducibility to date. Figure 12 shows the E_{corr} of Pt and Ni versus YSZ/Fe-Fe_3O_4 at 338°C, for different aqueous H_2 levels. This test has six phases: (A) 40 scc/kg H_2, (B) 19 scc/kg H_2, (C) 15 scc/kg H_2, (D) 10 scc/kg H_2, (E) 15 scc/kg H_2, and (F) 19 scc/kg H_2. The Pt and Ni E_{corr} values in phases (C) and (E) are very similar (*i.e.*, within ~ 2 mV). The Ni E_{corr} values in phase (B) are similar to the values in phase (F); a similar comparison cannot be made for Pt since the E_{corr} data for Pt did not have enough time to reach a steady-state value in phase (F). Additionally, different probes provide reproducible results. For example, E_{corr} values for Ni and Pt at 40 scc/kg H_2 are 0.203 and 0.206 V *vs.* Fe/Fe_3O_4, respectively, in one test conducted at 316°C. In a subsequent 316°C test with a different electrode, E_{corr} values for Ni and Pt at 40 scc/kg H_2 are 0.205 and 0.209 V *vs.* Fe/Fe_3O_4, respectively (Table 6).

Response time: The potentials measured versus the YSZ/Fe-Fe_3O_4 electrode show rapid response to changes in the aqueous hydrogen level. As an example, in Figure 12 the aqueous hydrogen level is changed at 67, 114, 234, 283 and 453 hours. The ECP response for both the platinum and nickel is evident on the subsequent data point (data taken ~ every 10 minutes) in most cases.

Impedance: The impedance of a RE must be low relative to the input impedance of the voltmeter, to prevent measurement errors due to 'loading' of the voltmeter. Because conductivity in the YSZ/Fe-

[5] Note that the equilibrium lines in the Pourbaix diagrams were constructed using a slightly different thermodynamic data set than the theoretical predictions of the hydrogen equilibrium potential *vs.* the YSZ/Fe-Fe_3O_4 electrode shown in Figures 5 (a) to 9 (a), and thus this comparison does constitute an independent check on the measurements.

Fe_3O_4 electrode depends on oxygen ion transport through the ceramic membrane, its impedance tends to be greater than that of traditional high temperature REs such as the Ag/AgCl electrode (whose conductivity depends on ion diffusion through water). Thus, the results of impedance measurements (Table 3) are compared to the input impedance of the voltmeters, as discussed below.

Table 3. Measured YSZ/Fe-Fe_3O_4 Electrode Impedance Values.

Temperature (°C)	Impedance between Fe/Fe_3O_4 electrode and the autoclave (kΩ)	Impedance between Fe/Fe_3O_4 electrode and a Pt wire (kΩ)	Impedance between Fe/Fe_3O_4 electrode and a Ni wire (kΩ)
282	120.5	110.7	106.1
338	17.8	25.4	25.5

As expected, the impedance values (Table 3) are higher at 282°C than at 338°C. The values are reasonably consistent with previously reported values [20], in which resistances of 100 and 88 kΩ were reported at 250°C. All voltmeters used for ECP measurements in this study have an input impedance of ≥ 10 GΩ (*i.e.*, ~ 10^5 X greater than the impedance of the YSZ probe at 282°C). These results provide confidence that probe impedance is not adversely affecting the ECP measurements.

Benefits: Method (3) is useful in off-nominal environments, the aqueous H_2 level does not have to be known, and the measured potentials are pH-independent since the Fe/Fe_3O_4 equilibrium has the same pH dependence as the hydrogen equilibrium. Also, the YSZ/Fe-Fe_3O_4 electrode is often sensitive to inadvertent chemistry changes during a test, since its potential is not sensitive to changes in oxidizing or reducing conditions. Measurement of potential versus the YSZ/Fe-Fe_3O_4 electrode may therefore show a response if there is inadvertent ingress of an oxidizing agent, for example.

Drawbacks: The YSZ/Fe-Fe_3O_4 REs suffer from durability limitations, since the ceramic tube is inherently brittle and is thus susceptible to fracture, particularly at locations of metal-to-ceramic contact. Differential thermal expansion and/or misalignment can cause stress at these contact locations, which can lead to fracture of the ceramic either during assembly or in the autoclave. An example of the ECP-time trace observed due to RE failure in an autoclave is shown in Figure 13. In this test (360°C, 90 scc/kg H_2 from 0 to 161 hours), the RE was functioning effectively until ~ 40 to 60 hours, at which point the absolute value of the measured E_{corr} began to decrease. It is believed that water in-leakage to the 'active area' of the RE disrupts the equilibrium between Fe and Fe_3O_4 if the powder becomes wet.[6]

Recent design modifications have improved the durability of the RE. The new design employs a teflon sealant (Figure 14), which eliminates the metal-to-ceramic contact within the sealant region. Historically, teflon sealants have been used successfully in tests conducted in simulated BWR environments [13], which are typically conducted at ~ 288°C. However, there has always been concern for using teflon sealants at higher temperatures such as those tested in the present study (*i.e.*, up to 360°C), since in order to use teflon, the sealant region must be kept to less than ~ 93°C. Recent testing has shown that such concerns are legitimate, but that this problem is not intractable. For example, to counteract the increase of sealant temperature, the REs are always placed through a bottom penetration of the autoclave. Also, the use of a 'stand-off' (*i.e.*, a 25.4 mm long tube fitting) to move the sealant further away from the autoclave has been successful in reducing the sealant temperature. If the temperature of the sealant increases, the Conax™ housing can be periodically re-

[6] Specifically, it is believed that wetting of the powder and the wire creates a mixed potential on the wire which is intermediate between the Fe/Fe_3O_4 potential and the hydrogen equilibrium potential associated with hydrogenated water.

torqued to counteract the extrusion of the teflon (note that the use of the stand-off has minimized the need for re-torque after autoclave cooldown).

An additional new design feature is that the annular gap between the outer diameter of the ceramic tube and the inner diameter of the Conax™ housing has been enlarged, such that more lateral displacement of the ceramic tube is permitted before metal-to-ceramic contact occurs. Thicker wall ceramic tube is also being used in some of the newer REs, which is expected to provide some increase in tube fracture resistance. Note that the standard size tube used in this work has a wall thickness of 0.81 mm, an outside diameter of 6.35 mm and a length of 279.4 to 304.8 mm. The thicker wall ceramic presently under evaluation has a wall thickness of 1.27 mm.

The YSZ/Fe-Fe_3O_4 electrode has a cost of ~ $650 per new electrode, primarily due to the price of custom-built Conax™ fittings required for the electrode pressure boundary, and to the yttria-stabilized zirconia tube. The cost of a replacement electrode is ~ $400, since the Conax™ housing can be reused (a new sealant and a new ceramic tube are needed for each replacement probe). Note that the time to assemble the probe is ~ 1 hour.

Hydrogen Fugacity Measurements using a Silver/Palladium Tube: Data from four tests are shown in Figure 15 (a). The steady-state pressure is a function of the aqueous H_2 concentration, as expected. The calculated pressures on the right side of Figure 15 (a) were determined using the Henry's Law coefficient from Table 1 (*i.e.*, 0.015 atm/(scc/kg)). Good agreement was obtained between the measured and calculated values, as shown in Figure 15 (b).

DISCUSSION: Converting Corrosion Potentials to the ECP *vs.* Ni/NiO scale

As described previously [2-7], a maximum in SCC growth rate for nickel-based alloys occurs near the measured Ni/NiO phase transition, as shown in Figures 1 and 16. Thus, the ECP of a specimen or component versus the ECP of the Ni/NiO transition is believed to be the correct parameter for describing aqueous H_2 effects on PWSCC [3, 4, 8]. The following section describes how to determine this "ECP difference" (*i.e.*, $ECP_{Ni\text{-}alloy} - ECP_{Ni/NiO}$ or, alternatively, $ECP_{Ni/NiO} - ECP_{Ni\text{-}alloy}$).

Using Method 1: As shown earlier, nickel-based alloys essentially behave as hydrogen electrodes at ≥ ~ 5 to 10 scc/kg H_2. Thus, the respective aqueous H_2 levels for the environment of interest and the Ni/NiO transition, $[H_2]_{environment}$ and $[H_2]_{Ni/NiO}$, respectively, can be related to ECP via the Nernst equation. Therefore, the ECP of the specimen can be calculated using equation [2]:

$$ECP^{SHE}_{Ni-alloy} = -\frac{RT}{nF}\left\{\ln\left(\left[H_2\right]_{environment} \cdot H\right) + 4.6 \cdot pH\right\}\,[Volts] \qquad [9]$$

and the ECP of the Ni/NiO transition can be calculated using the Nernst equation for a hydrogen electrode at the aqueous H_2 level of the transition (*i.e.*, $[H_2]_{Ni/NiO}$)[7]:

$$ECP^{SHE}_{Ni/NiO} = -\frac{RT}{nF}\left\{\ln\left(\left[H_2\right]_{Ni/NiO} \cdot H\right) + 4.6 \cdot pH\right\}[Volts] \qquad [10]$$

[7] In a Pourbaix diagram, the Ni/NiO phase transition (single line) and hydrogen electrodes (multiple lines as a function of H_2 level) have the same slope. These lines are common at the H_2 concentration of the Ni/NiO transition. The aqueous H_2 levels for the measured Ni/NiO transition at 288, 316, 338 and 360°C are 4, 7.5, 13.8 and 25 scc/kg H_2, respectively [7].

The "ECP difference" (*i.e.*, ΔECP) between the specimen and the Ni/NiO phase transition is:

$$\Delta ECP = ECP^{SHE}_{Ni/NiO} - ECP^{SHE}_{Ni-alloy} = 4.3x10^{-5} \cdot T \left\{ \ln\left(\frac{[H_2]_{environment}}{[H_2]_{Ni/NiO}} \right) \right\} [Volts] \qquad [11]$$

Note that the terms involving H (Henry's law coefficient) and pH have dropped out, and that R/nF equals 4.3 x 10^{-5} in Volts/Kelvin, for this reaction. Equation [11] is simply the difference between two hydrogen electrodes, and only the temperature, aqueous H_2 level of the environment, and the aqueous H_2 level of the Ni/NiO phase transition [7] are needed to determine the "ECP difference".

<u>*Using Method 2*</u>: The ECP difference using this method can be written as:

$$\Delta ECP = ECP_{Ni/NiO} - ECP_{Ni-alloy} = \left\{ ECP^{SHE}_{Ni/NiO} - ECP^{SHE}_{Pt} \right\} - \left\{ ECP_{Ni-alloy} - ECP_{Pt} \right\} [Volts] \; [12]$$

Assuming that the Pt behaves as a hydrogen electrode, the term in the first brackets is simply:

$$ECP_{Ni/NiO} - ECP_{Pt} = 4.3x10^{-5} \cdot T \left\{ \ln\left(\frac{[H_2]_{environment}}{[H_2]_{Ni/NiO}} \right) \right\} [Volts] \qquad [13]$$

and the second term is the measured steady-state voltage between the Ni-alloy and the Pt electrode (*i.e.*, $ECP_{Ni\text{-}alloy} - ECP_{Pt}$). This term in the second brackets of equation [12] corrects for the extent that the specimen ECP departs from that of a true hydrogen electrode. This value is subtracted from equation [13], to calculate the final ECP difference:

$$ECP_{Ni/NiO} - ECP_{Ni-alloy} = 4.3x10^{-5} \cdot T \left\{ \ln\left(\frac{[H_2]_{environment}}{[H_2]_{Ni/NiO}} \right) \right\} - \left[ECP_{specimen} - ECP_{Pt} \right] [Volts] \; [14]$$

As shown in Figure 3, this correction becomes appreciable only at low H_2 levels (< ~ 5 to 10 scc/kg).

As an example, consider an Alloy 600 specimen tested at 338°C and 120 scc/kg H_2. The measured value of $[ECP_{specimen} - ECP_{Pt}]$ was – 2 mV in this test (Figure 3). At 338°C, the measured Ni/NiO phase transition is located at 13.8 scc/kg H_2 [7]. Thus, the "ECP difference" is:

$$\Delta ECP = ECP_{Ni/NiO} - ECP_{Ni-alloy} = 4.3x10^{-5} \cdot 611 \left\{ \ln\left(\frac{120}{13.8} \right) \right\} - [-2] = 0.059 \, Volts = 59 \, mV \; [15]$$

Figure 16 shows that the ECP difference for the 120 scc/kg H_2 point at 338°C is located at 59 mV.

<u>*Using Method 3*</u>: In this case, the ECP difference (*i.e.*, $ECP_{Ni/NiO} - ECP_{Ni\text{-}alloy}$ or ΔECP) is:

$$ECP_{Ni/NiO} - ECP_{Ni-alloy} = \{ECP^{SHE}_{Ni/NiO} - ECP^{SHE}_{Fe-Fe_3O_4}\} - \{ECP_{Ni-alloy} - ECP_{Fe-Fe_3O_4}\}\ [Volts] \quad [16]$$

The term in the first brackets can be determined by subtracting equation [6] from equation [10], and the term in the second brackets is the measured steady-state voltage between the test specimen and the YSZ RE. This equation can be simplified to:

$$\Delta ECP = \frac{RT}{2F}\ln([H_2]_{Ni/NiO} \cdot H) - E^{o}_{Fe/Fe_3O_4} - \{ECP_{Ni-alloy} - ECP_{Fe-Fe_3O_4}\}\ [Volts] \quad [17]$$

A graphical method for determining this difference can also be used, by employing Figure 17 [7], which shows the Ni/NiO transition measurements in ECP space. Figure 17 shows that ECP measurements *vs.* the YSZ/Fe-Fe_3O_4 RE can discern whether a given environment is located in the Ni or NiO stability regime, and can quantify the ECP distance from this phase transition.

CONCLUSIONS

- Three methods are used to measure and calculate the electrochemical corrosion potential of nickel-base alloys in hydrogenated water (*e.g.*, ~ 1 to 150 scc/kg H_2) at 260 to 360°C.
  - The first method assumes that the specimen or component behaves as a hydrogen electrode, and its E_{corr} is calculated using the Nernst equation. The present work has shown that this method is valid for aqueous H_2 levels ≥ ~ 5 to 10 scc/kg H_2. This method provides the simplest approach for calculating E_{corr} for plant components or historical test specimens.
  - The second method utilizes a voltage measurement between the specimen or component and a Pt electrode, with the Pt assumed to behave as a hydrogen electrode. This method is valid even at H_2 levels < ~ 5 to 10 scc/kg, as long as the aqueous H_2 level is known. This method is judged to provide the best available approach for E_{corr} measurements in most cases.
  - The third method uses a voltage measurement versus a YSZ/Fe-Fe_3O_4 electrode. This work shows that the electrochemical performance of this electrode supports its viability as a RE in high temperature hydrogenated water. This method is the best approach if the H_2 level is unknown, or in off-nominal chemistries. Recent design modifications have improved the durability of the RE, though some of the REs do fail prematurely due to water in-leakage.
- Limited test data using a Ag/Pd tube at 260°C show that measured autoclave hydrogen pressures were consistent with the expected pressure values based on Henry's Law.
- Combining the three ECP methods described above with a Ag/Pd tube for measuring autoclave hydrogen pressures appears to provide an optimal method for environmental definition.
- Relating ECP to the Ni/NiO phase transition by the methods described above is advantageous for evaluating the SCC behavior of Ni-based alloys.

ACKNOWLEDGEMENTS

Thanks to Dr. James Orr, John Schisano and Nelson Schwarting. Also, the idea for using the iron/iron oxide probe as a reference electrode was adopted from Leonard Niedrach of GE-CRD.

REFERENCES

[1] G Economy and PW Pement, CORROSION/89, Paper No. 493, 1989.

[2] T Cassagne, F Vaillant, P Combrade, *Proceedings of the Eighth International Symposium on the Environmental Degradation of Materials in Nuclear Power Systems*, August 1997, p. 307.

[3] PM Scott, "Prediction of Alloy 600 Component Failures in PWR Systems", Proceedings of the Research Topical Symposium at CORROSION/96, 1999, p. 135.

[4] DS Morton, SA Attanasio, JS Fish and MK Schurman, CORROSION/99, Paper No. 447, 1999.

[5] N Totsuka, S Sakai, N Nakajima and H Mitsuda, CORROSION/2000, Paper No. 212, 2000.

[6] TB Cassagne and A Gelpi, from *Proceedings of the International Symposium on Plant Aging and Life Predictions of Corrodible Structures*, Sapporo, Japan, May 15 – 18, 1995, p. 921.

[7] SA Attanasio, DS Morton, MA Ando, NF Panayotou and CD Thompson, from *Proceedings of the Tenth International Symposium on the Environmental Degradation of Materials in Nuclear Power Systems*, Lake Tahoe, Nevada, August 2001.

[8] DS Morton, SA Attanasio and GA Young, *Proceedings of the Tenth International Symposium on the Environmental Degradation of Materials in Nuclear Power Systems*, Lake Tahoe, Nevada, August 2001.

[9] DD MacDonald, *J. Electrochem. Soc.*, Vol. 128, No. 2, February 1981, p. 250.

[10] S Hettiarachchi, SJ Lenhart and DD MacDonald, EPRI Report NP-5193, May 1987.

[11] S Hettiarachchi and DD MacDonald, *J. Electrochem. Soc.*, Vol. 131, No. 9, p. 2206.

[12] LW Niedrach, *J. Electrochem. Soc.*, Vol. 129, No. 7, July 1982, p. 1445.

[13] YJ Kim and PL Andresen, CORROSION/2001, Paper No. 137, 2001.

[14] YJ Kim, CORROSION/96, Paper No. 102, 1996.

[15] SE Ziemniak, *J. Sol. Chem.*, Vol. 21, No. 8, 1992.

[16] DS Morton, D Gladding, MK Schurman and CD Thompson, from *Proceedings of the Eighth International Symposium on the Environmental Degradation of Materials in Nuclear Power Systems*, Amelia Island, FL, August 1997, p. 387.

[17] SA Attanasio, JS Fish, WW Wilkening, PM Rosecrans, DS Morton, GS Was and Y Yi, from *Proceedings of the Ninth International Symposium on the Environmental Degradation of Materials in Nuclear Power Systems*, Newport Beach, California, August 1999, p. 49.

[18] DD MacDonald, *Corrosion*, Vol. 34, No. 3, March 1978, p. 75.

[19] SE Ziemniak, ME Jones and KES Combs, *J. Solution Chem.*, Vol. 24, No. 9, 1995.

[20] S Hettiarachchi, P Kedzierzawski and DD MacDonald, *J. Electrochem. Soc.*, Vol. 132, No. 8, August 1985.

Table 4. Electrochemical Corrosion Potential (ECP) Data at 260°C for Pt and Alloy X-750 Condition AH (AH) [4].

$[H_2]$ (scc/kg)	Measured E_{corr} of Pt vs. Fe/Fe_3O_4 (V)	Measured E_{corr} of Pt vs. SHE (V) [1,2]	$[H_2]$ (scc/kg)	Measured E_{corr} of AH vs. Fe/Fe_3O_4 (V)	Measured E_{corr} of AH vs. SHE (V) [1,2]	$[H_2]$ (scc/kg)	Theoretical $E_{hydrogen\ electrode}$ vs. Fe/Fe_3O_4 (V) [3]	Theoretical $E_{hydrogen\ electrode}$ vs. SHE (V) [4]
0.7	0.306	-0.573	0.7	0.241	-0.638	1	0.269	-0.610
5	0.206	-0.673	5	0.190	-0.689	5	0.232	-0.647
20	0.189	-0.690	20	0.190	-0.689	10	0.216	-0.663
106	0.154	-0.725	106	0.156	-0.723	15	0.207	-0.672
-	-	-	-	-	-	20	0.200	-0.679
-	-	-	-	-	-	25	0.195	-0.684
-	-	-	-	-	-	30	0.191	-0.688
-	-	-	-	-	-	40	0.184	-0.695
-	-	-	-	-	-	50	0.179	-0.700
-	-	-	-	-	-	60	0.175	-0.704
-	-	-	-	-	-	70	0.172	-0.707
-	-	-	-	-	-	80	0.168	-0.711
-	-	-	-	-	-	90	0.166	-0.713
-	-	-	-	-	-	100	0.163	-0.716
-	-	-	-	-	-	110	0.161	-0.718
-	-	-	-	-	-	120	0.159	-0.720

[1] Data measured vs. the YSZ/Fe-Fe_3O_4 electrode (*i.e.*, Fe/Fe_3O_4) were converted to the SHE scale by subtracting 0.879 V (Table 2).
[2] A slightly different SHE conversion (0.880 Volts) was employed in [4], where the AH and Pt data were initially reported. All data points reported in the present document were converted using the updated Fe/Fe_3O_4-to-SHE conversion (*i.e.*, 0.879 V at 260°C).
[3] The theoretical hydrogen electrode values vs. SHE were converted to the Fe/Fe_3O_4 scale by adding 0.879 V (Table 2).
[4] Theoretical hydrogen electrode values on the SHE scale were calculated using Equation [2] and Table 1.

Table 5. ECP Data at 288°C for Pt and Nickel (Ni).

$[H_2]$ (scc/kg)	Measured E_{corr} of Pt vs. Fe/Fe_3O_4 (V)	Measured E_{corr} of Pt vs. SHE (V) [1]	$[H_2]$ (scc/kg)	Measured E_{corr} of Ni vs. Fe/Fe_3O_4 (V)	Measured E_{corr} of Ni vs. SHE (V) [1]	$[H_2]$ (scc/kg)	Theoretical $E_{hydrogen\ electrode}$ vs. Fe/Fe_3O_4 (V) [2]	Theoretical $E_{hydrogen\ electrode}$ vs. SHE (V) [3]
3	0.236	-0.680	3	0.234	-0.682	1	-0.291	-0.625
5	0.224	-0.692	5	0.223	-0.693	5	0.252	-0.664
5	0.219	-0.697	5	0.227	-0.689	10	0.236	-0.680
10	0.210	-0.706	5	0.220	-0.696	15	0.226	-0.690
10	0.208	-0.708	10	0.211	-0.705	20	0.219	-0.697
10	0.215	-0.701	10	0.209	-0.707	25	0.213	-0.703
-	-	-	10	0.208	-0.708	30	0.209	-0.707
-	-	-	19	0.196	-0.720	40	0.202	-0.714
-	-	-	-	-	-	50	0.197	-0.719
-	-	-	-	-	-	60	0.192	-0.724
-	-	-	-	-	-	70	0.189	-0.727
-	-	-	-	-	-	80	0.185	-0.731
-	-	-	-	-	-	90	0.183	-0.733
-	-	-	-	-	-	100	0.180	-0.736
-	-	-	-	-	-	110	0.178	-0.738
-	-	-	-	-	-	120	0.176	-0.740

[1] Data measured vs. the YSZ/Fe-Fe_3O_4 electrode (*i.e.*, Fe/Fe_3O_4) were converted to the SHE scale by subtracting 0.916 V (Table 2).
[2] The theoretical hydrogen electrode values vs. SHE were converted to the Fe/Fe_3O_4 scale by adding 0.916 V (Table 2).
[3] Theoretical hydrogen electrode values on the SHE scale were calculated using Equation [2] and Table 1.

Table 6. ECP Data at 316°C for Pt, Ni, and Alloy 600 (A600) (from the present study and [4]).

$[H_2]$ (scc/kg)	Measured E_{corr} of Pt vs. Fe/Fe_3O_4 (V)	Measured E_{corr} of Pt vs. SHE (V) [1]	$[H_2]$ (scc/kg)	Measured E_{corr} of Ni or A600 vs. Fe/Fe_3O_4 (V)	Measured E_{corr} of Ni or A600 vs. SHE (V) [1]	$[H_2]$ (scc/kg)	Theoretical $E_{hydrogen\ electrode}$ vs. Fe/Fe_3O_4 (V) [2]	Theoretical $E_{hydrogen\ electrode}$ vs. SHE (V) [3]
5	0.247	-0.702	5	0.246	-0.703	1	0.314	-0.635
5	0.249	-0.700	5	0.245	-0.704	5	0.274	-0.675
5	0.251	-0.698	5	0.246	-0.703	10	0.256	-0.693
5	0.252	-0.697	5	0.247	-0.702	15	0.246	-0.703
10	0.234	-0.715	10	0.231	-0.718	20	0.239	-0.710
10	0.234	-0.715	10	0.231	-0.718	25	0.233	-0.716
10	0.236	-0.713	10	0.231	-0.718	30	0.228	-0.721
10	0.238	-0.711	10	0.233	-0.716	40	0.221	-0.728
15	0.225	-0.724	15	0.223	-0.726	50	0.215	-0.734
15	0.227	-0.722	15	0.222	-0.727	60	0.211	-0.738
15	0.228	-0.721	15	0.222	-0.727	70	0.207	-0.742
20	0.218	-0.731	20	0.216	-0.733	80	0.203	-0.746
20	0.219	-0.730	20	0.216	-0.733	90	0.200	-0.749
20	0.218	-0.731	20	0.216	-0.733	100	0.198	-0.751
25	0.216	-0.733	20	0.215	-0.734	110	0.195	-0.754
30	0.212	-0.737	25	0.214	-0.735	120	0.193	-0.756
40	0.203	-0.746	30	0.211	-0.738	-	-	-
40	0.209	-0.740	40	0.205	-0.746	-	-	-
40	0.207	-0.742	40	0.200	-0.749	-	-	-
40	0.206	-0.743	40	0.203	-0.744	-	-	-
60	0.197	-0.752	40	0.203	-0.746	-	-	-
-	-	-	60	0.193	-0.756	-	-	-
-	-	-	120	0.177 (A600)	-0.772 (A600)	-	-	-

[1] Data measured vs. the YSZ/Fe-Fe_3O_4 electrode (*i.e.*, Fe/Fe_3O_4) were converted to the SHE scale by subtracting 0.949 V (Table 2).
[2] The theoretical hydrogen electrode values vs. SHE were converted to the Fe/Fe_3O_4 scale by adding 0.949 V (Table 2).
[3] Theoretical hydrogen electrode values on the SHE scale were calculated using Equation [2] and Table 1.

Table 7. ECP Data at 338°C for Pt, Ni, and Alloy X-750 Condition AH (AH) (from the present study and [4]).

$[H_2]$ (scc/kg)	Measured E_{corr} of Pt vs. Fe/Fe_3O_4 (V)	Measured E_{corr} of Pt vs. SHE (V) [1,2]	$[H_2]$ (scc/kg)	Measured E_{corr} of Ni or AH vs. Fe/Fe_3O_4 (V)	Measured E_{corr} of Ni or AH vs. SHE (V) [1,2]	$[H_2]$ (scc/kg)	Theoretical $E_{hydrogen\ electrode}$ vs. Fe/Fe_3O_4 (V) [3]	Theoretical $E_{hydrogen\ electrode}$ vs. SHE (V) [4]
0.7	0.313	-0.677	0.7	0.266	-0.724	1	0.335	-0.655
5	0.274	-0.716	5	0.258	-0.732	5	0.292	-0.698
20	0.240	-0.750	20	0.236	-0.754	10	0.274	-0.716
40	0.224	-0.766	40	0.222 (Ni)	-0.768 (Ni)	15	0.264	-0.726
40	0.223	-0.767	40	0.222 (Ni)	-0.768 (Ni)	20	0.256	-0.734
106	0.203	-0.787	106	0.200	-0.790	25	0.250	-0.740
-	-	-	-	-	-	30	0.245	-0.745
-	-	-	-	-	-	40	0.238	-0.752
-	-	-	-	-	-	50	0.232	-0.758
-	-	-	-	-	-	60	0.227	-0.763
-	-	-	-	-	-	70	0.223	-0.767
-	-	-	-	-	-	80	0.220	-0.770
-	-	-	-	-	-	90	0.217	-0.773
-	-	-	-	-	-	100	0.214	-0.776
-	-	-	-	-	-	110	0.211	-0.779
-	-	-	-	-	-	120	0.209	-0.781

[1] Data measured vs. the YSZ/Fe-Fe_3O_4 electrode (*i.e.*, Fe/Fe_3O_4) were converted to the SHE scale by subtracting 0.990 V (Table 2).
[2] A slightly different SHE conversion (0.993 Volts) was employed in [4], where the AH and Pt data were initially reported. All data points reported in the present document were converted using the updated Fe/Fe_3O_4-to-SHE conversion (*i.e.*, 0.990 V at 338°C).
[3] The theoretical hydrogen electrode values vs. SHE were converted to the Fe/Fe_3O_4 scale by adding 0.990 V (Table 2).
[4] Theoretical hydrogen electrode values on the SHE scale were calculated using Equation [2] and Table 1.

Table 8. ECP Data at 360°C for Pt, Ni, and Alloy X-750 Condition HTH (HTH) (from the present study and [4]).

$[H_2]$ (scc/kg)	Measured E_{corr} of Pt vs. Fe/Fe_3O_4 (V)	Measured E_{corr} of Pt vs. SHE (V) [1,2]	$[H_2]$ (scc/kg)	Measured E_{corr} of Ni or HTH vs. Fe/Fe_3O_4 (V)	Measured E_{corr} of Ni or HTH vs. SHE (V) [1,2]	$[H_2]$ (scc/kg)	Theoretical $E_{hydrogen\ electrode}$ vs. Fe/Fe_3O_4 (V) [3]	Theoretical $E_{hydrogen\ electrode}$ vs. SHE (V) [4]
1	0.332	-0.716	1	0.300	-0.748	1	0.357	-0.691
6	0.295	-0.753	6	0.288	-0.760	5	0.313	-0.735
21	0.256	-0.792	21	0.253	-0.795	10	0.294	-0.754
30	0.247	0.801	30	0.243	-0.805	15	0.283	-0.765
90	0.222	-0.826	90	0.219 (Ni)	-0.829 (Ni)	20	0.275	-0.773
-	-	-	-	-	-	25	0.269	-0.779
-	-	-	-	-	-	30	0.264	-0.784
-	-	-	-	-	-	40	0.257	-0.791
-	-	-	-	-	-	50	0.251	-0.797
-	-	-	-	-	-	60	0.246	-0.802
-	-	-	-	-	-	70	0.241	-0.807
-	-	-	-	-	-	80	0.238	-0.810
-	-	-	-	-	-	90	0.235	-0.813
-	-	-	-	-	-	100	0.232	-0.816
-	-	-	-	-	-	110	0.229	-0.819
-	-	-	-	-	-	120	0.227	-0.821

[1] Data measured vs. the YSZ/Fe-Fe_3O_4 electrode (*i.e.*, Fe/Fe_3O_4) were converted to the SHE scale by subtracting 1.048 V (Table 2).

[2] A slightly different SHE conversion (1.068 Volts) was employed in [4], where the HTH and Pt data were initially reported. All data points reported in this document were converted using the updated Fe/Fe_3O_4-to-SHE conversion (*i.e.*, 1.048 V at 360°C).

[3] The theoretical hydrogen electrode values vs. SHE were converted to the Fe/Fe_3O_4 scale by adding 1.048 V (Table 2).

[4] Theoretical hydrogen electrode values on the SHE scale were calculated using Equation [2] and Table 1.

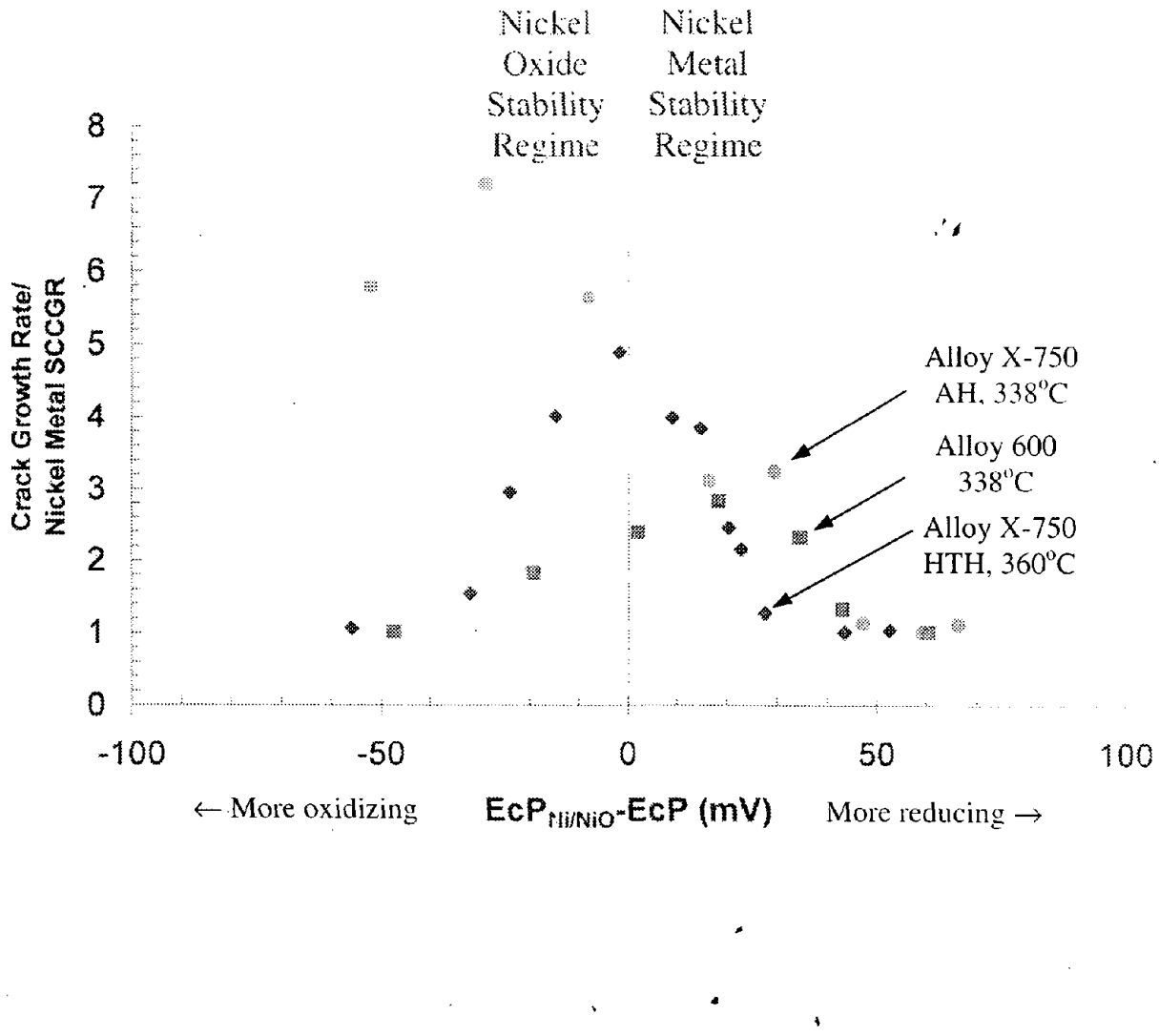

Figure 1. Normalized stress corrosion crack growth rate (SCCGR) for several nickel-based alloys at 338 and 360°C, plotted as a function of electrochemical potential (ECP) relative to the ECP of the Ni/NiO phase transition [8]. Crack growth rates are normalized to the minimum growth rate measured for each material (*i.e.*, ~ 0.64 μm/hr for Alloy X-750 in the AH heat treatment at 338°C, ~ 0.34 μm/hr for Alloy X-750 HTH at 360°C, and ~ 0.16 μm/hr for Alloy 600 at 338°C).

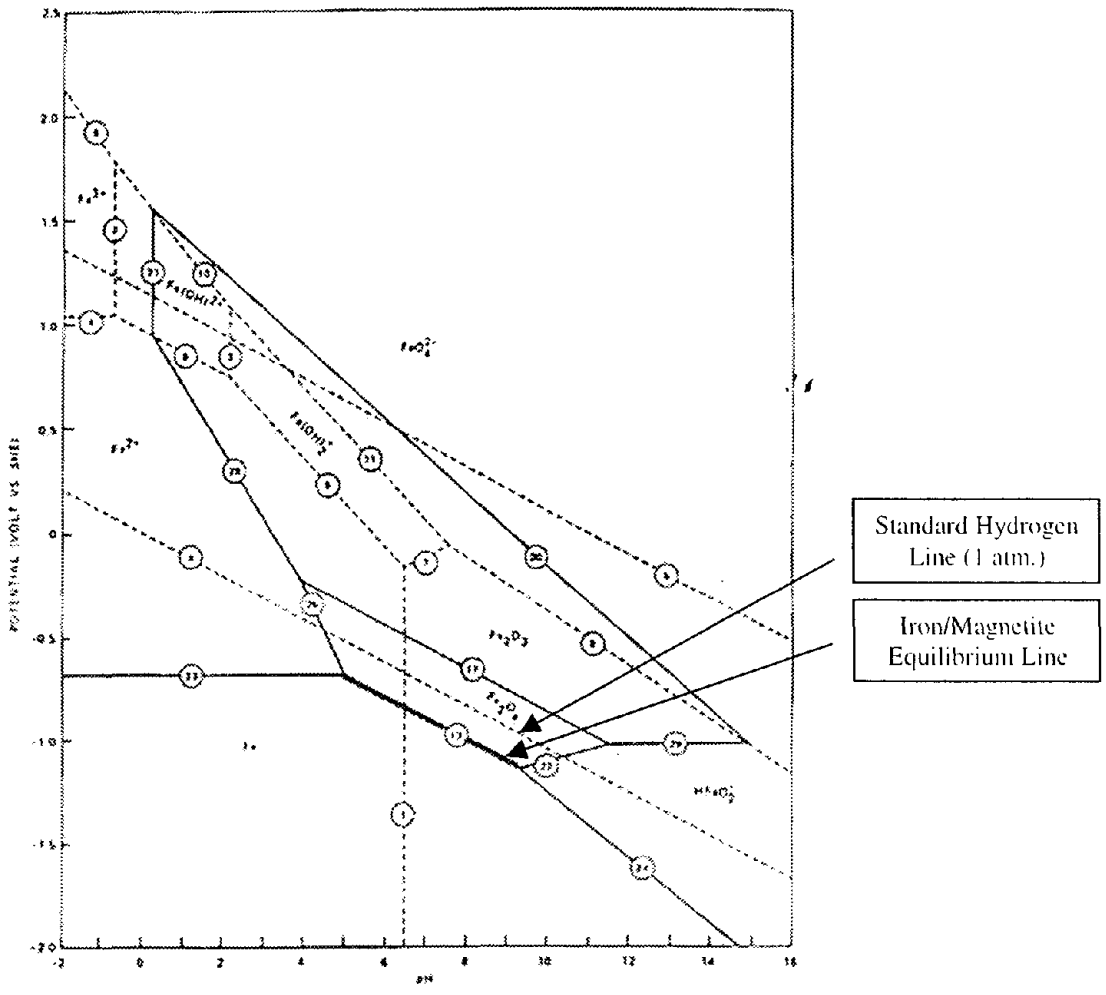

Figure 2. Pourbaix diagram for iron (Fe) at 250°C [EPRI].

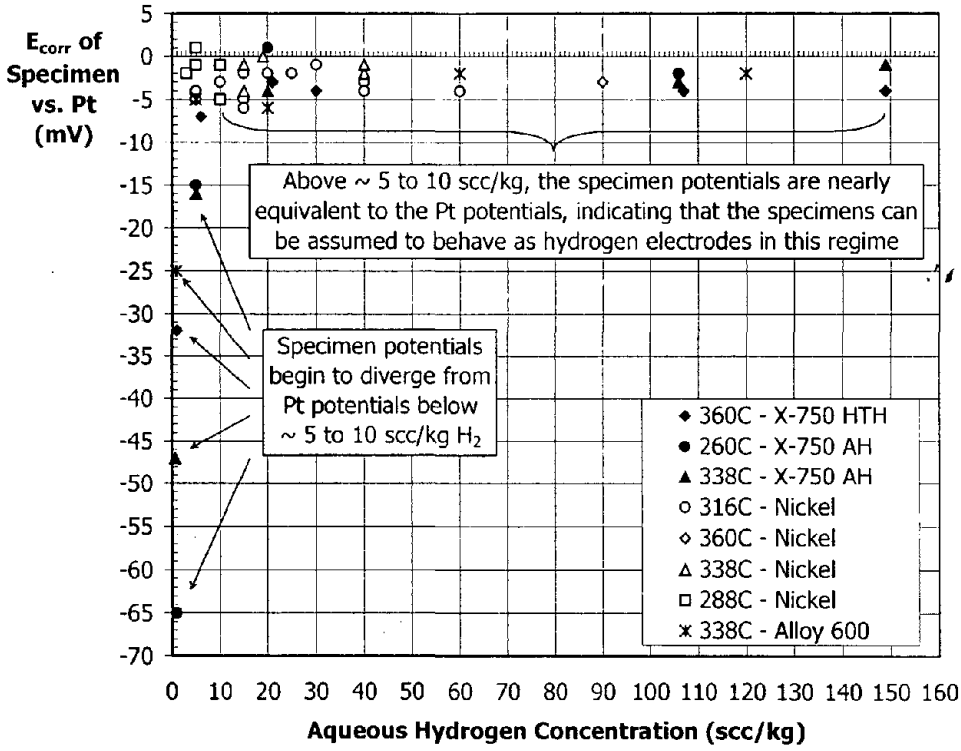

Figure 3. Electrochemical corrosion potential (E_{corr}) of nickel and several types of Ni-based alloy specimens versus a platinum electrode as a function of aqueous hydrogen concentration, at 260, 288, 316, 338, and 360°C.

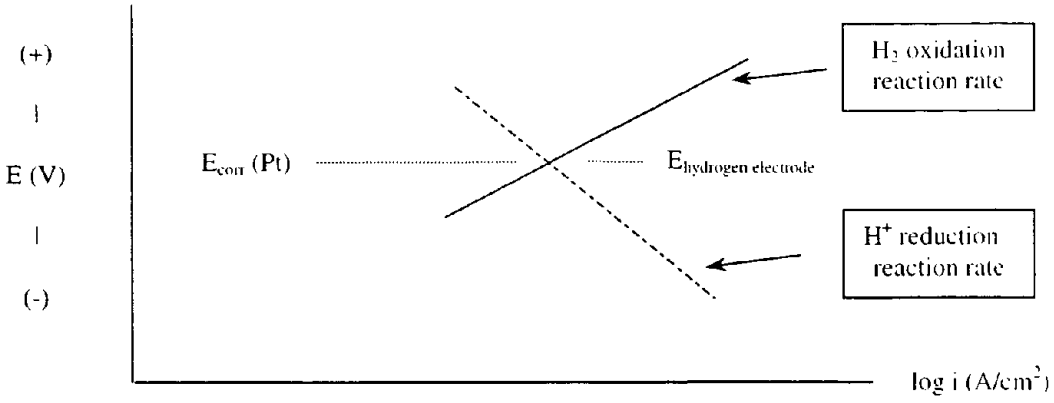

Figure 4 (a). Schematic Evans diagram for Pt in hydrogenated water. The intersection of the reaction rate curves for the H_2 oxidation and H^+ reduction reactions corresponds to the ECP of a hydrogen electrode. The Pt ECP is that of a hydrogen electrode.

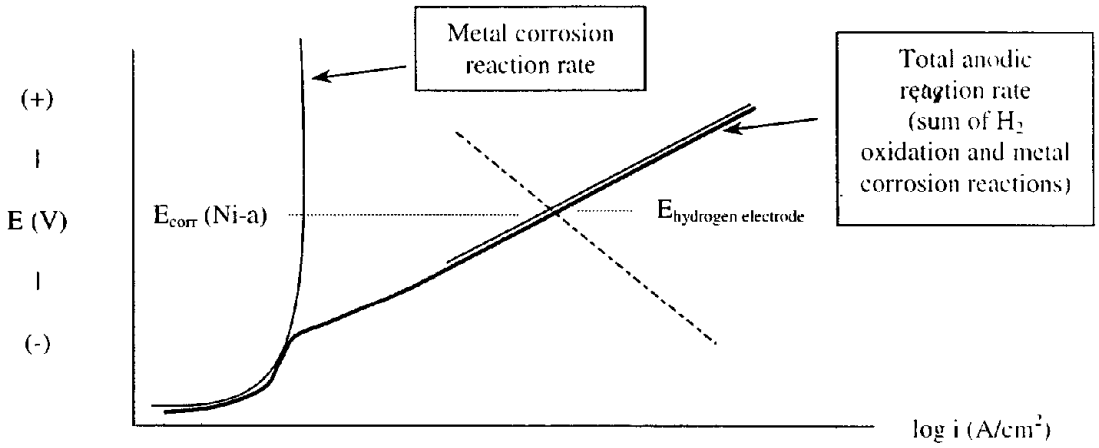

Figure 4 (b). Schematic Evans diagram for Ni-based alloys at relatively high aqueous H_2 levels. The total anodic reaction rate is dominated by H_2 oxidation. Thus, the E_{corr} of the Ni-based alloys (Ni-a) is negligibly different from that of a hydrogen electrode.

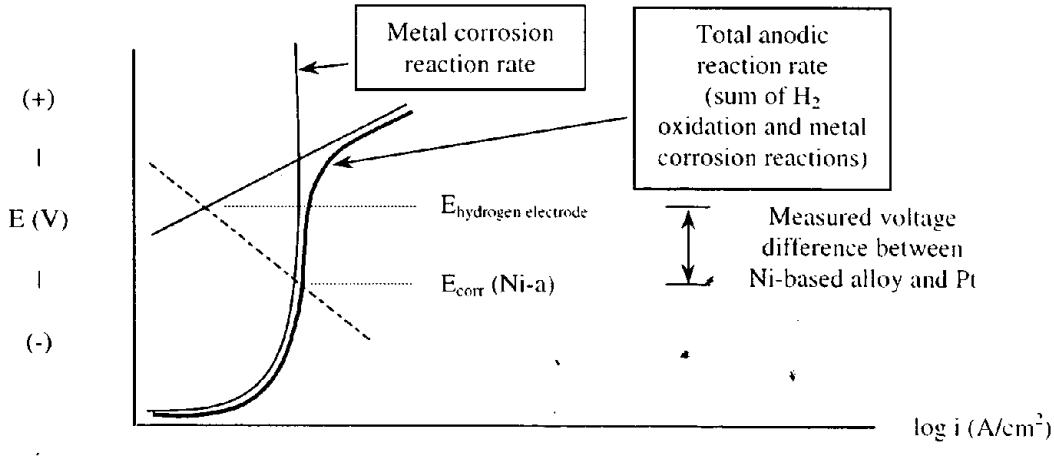

Figure 4 (c). Schematic Evans diagram for Ni-based alloys at low aqueous H_2 levels. The total anodic reaction rate is now influenced by metal corrosion. Thus, the E_{corr} of the Ni-based alloys (Ni-a) is appreciably lower than that of a hydrogen electrode.

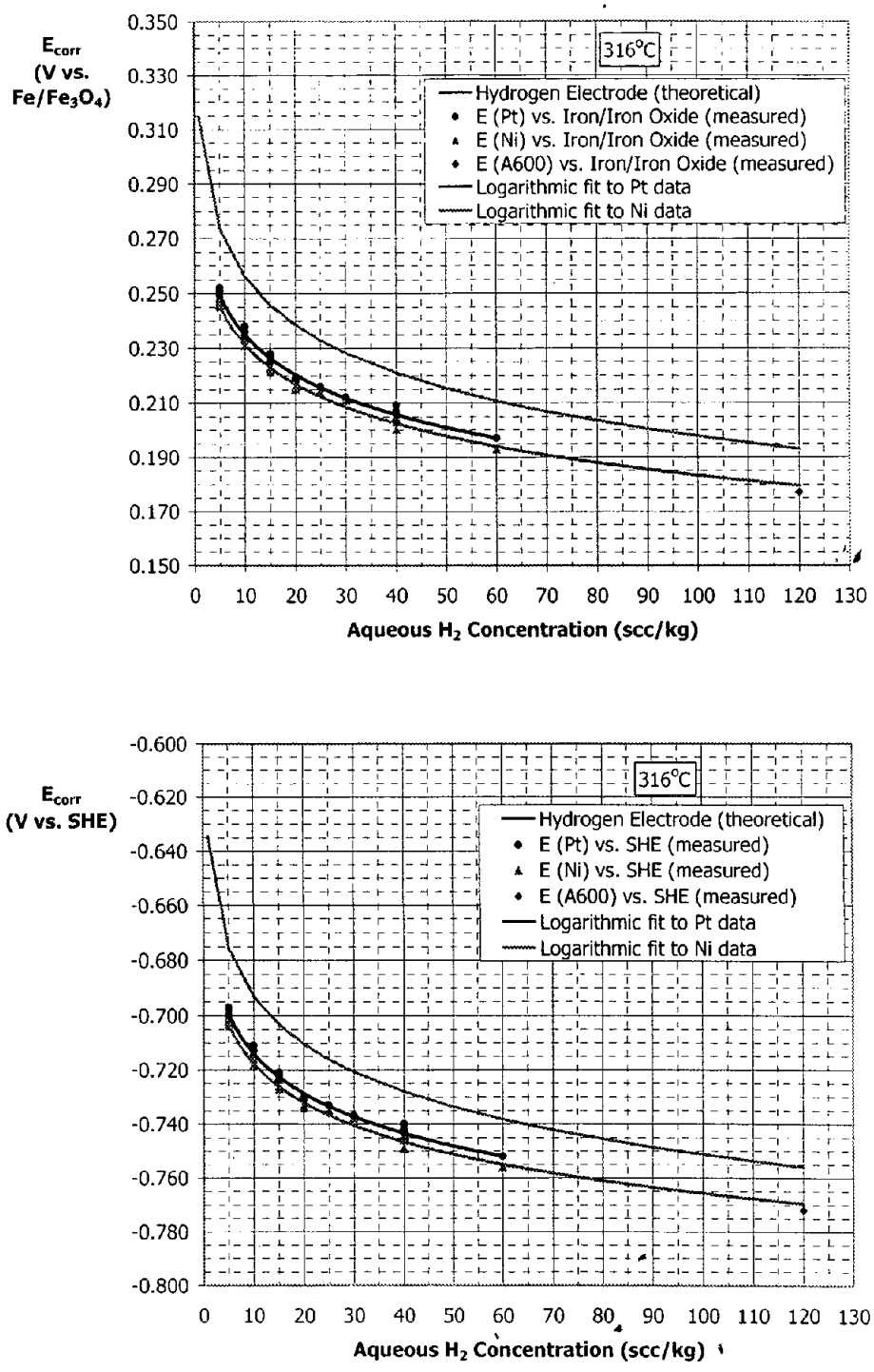

Figure 5. Electrochemical corrosion potentials (E_{corr}) at 316°C for platinum, nickel, and Alloy-600 as well as the theoretical hydrogen electrode potential, vs. the iron/iron oxide RE (a) and the standard hydrogen electrode (SHE) scale (b), as a function of aqueous hydrogen concentration. Logarithmic fits to the Pt and Ni data are also included. Logarithmic fits were selected due to the apparent agreement of the data with Nernstian behavior.

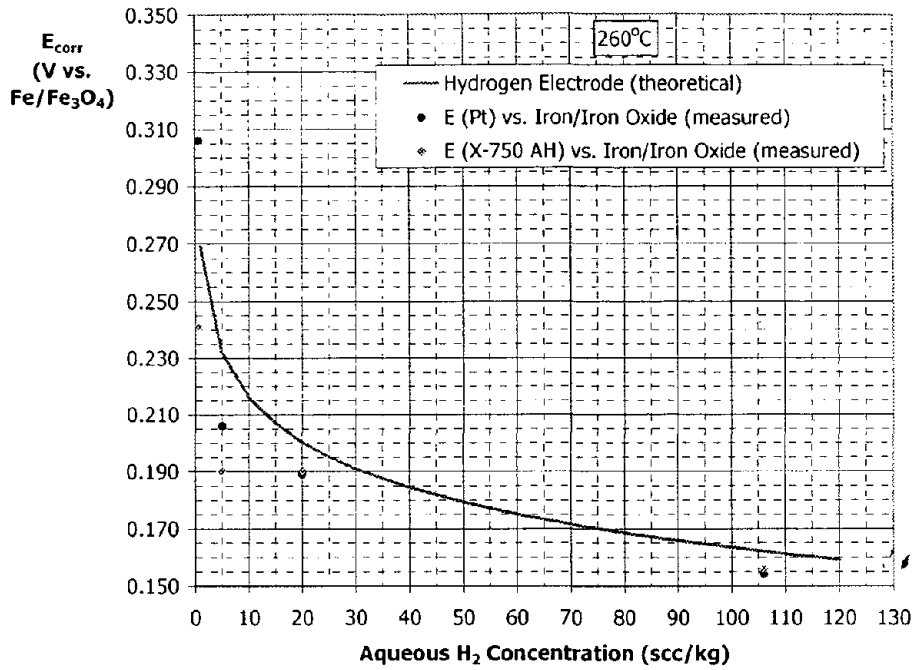

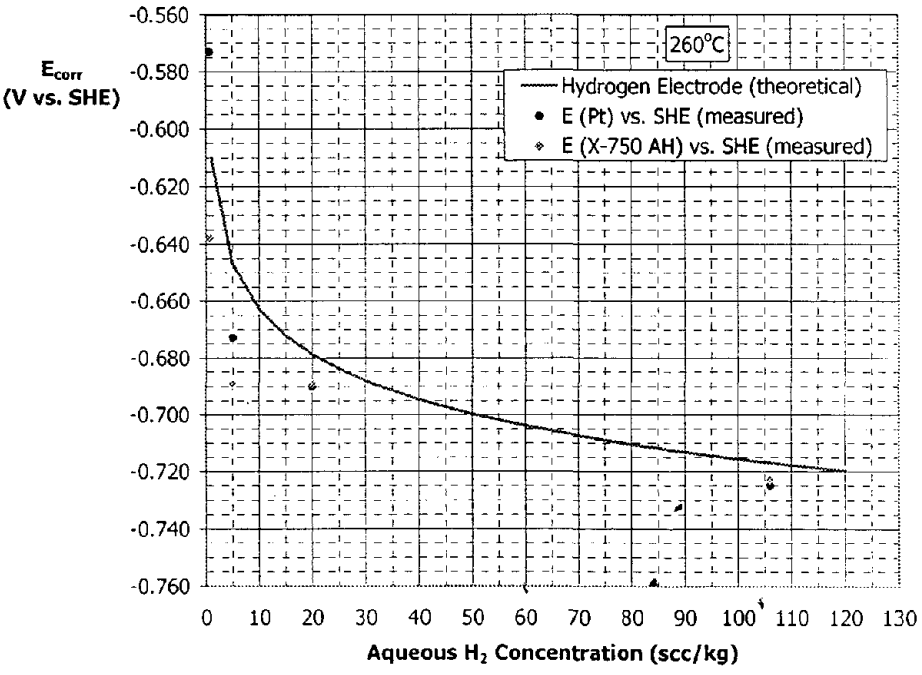

Figure 6. Electrochemical corrosion potentials (E_{corr}) at 260°C for platinum and Alloy X-750 in the AH heat treatment (X-750 AH) as well as the theoretical hydrogen electrode potential, *vs.* the iron/iron oxide RE (a) and the standard hydrogen electrode (SHE) scale (b), as a function of aqueous hydrogen concentration.

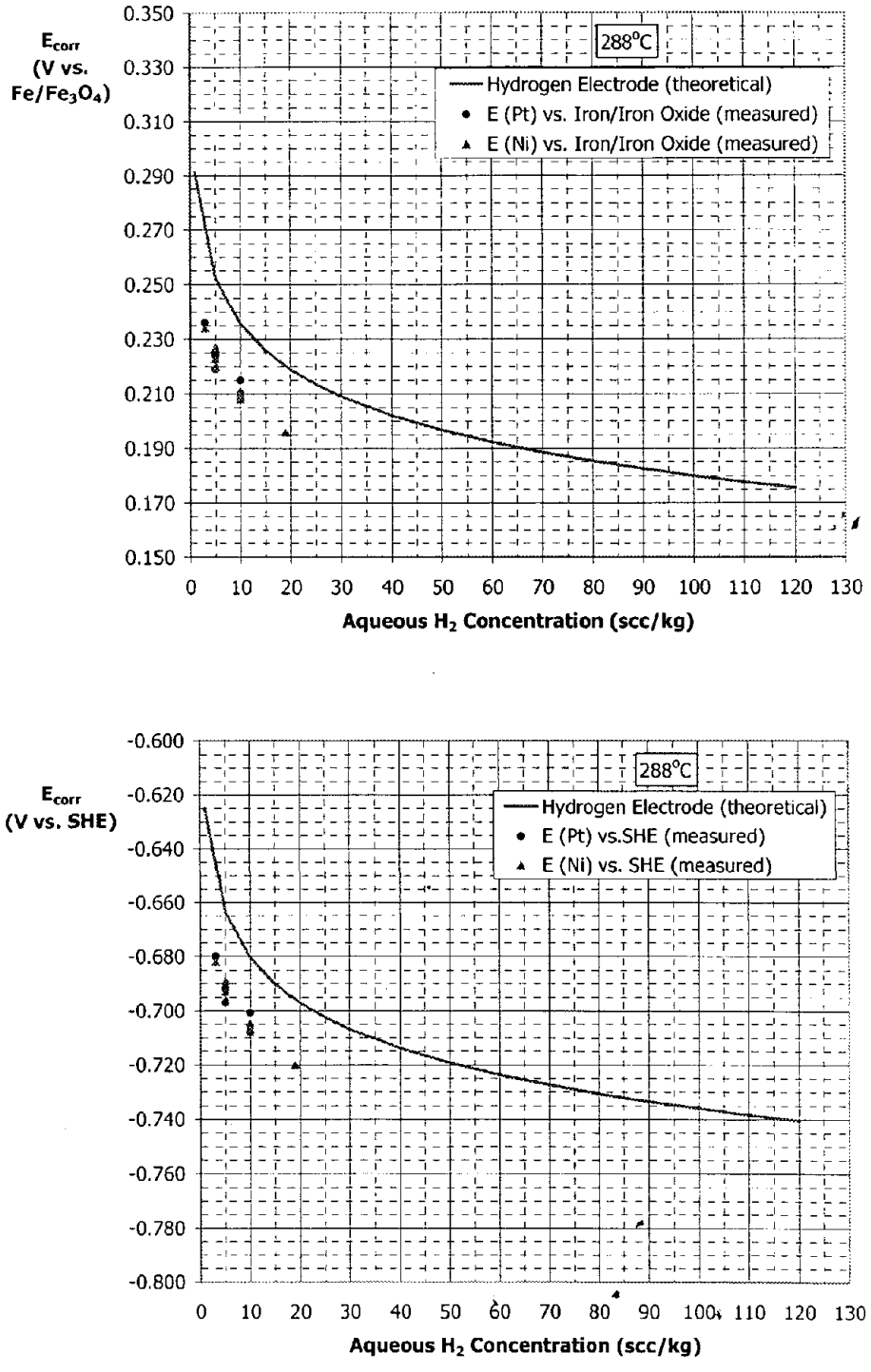

Figure 7. Electrochemical corrosion potentials (E_{corr}) at 288°C for platinum and nickel as well as the theoretical hydrogen electrode potential, *vs.* the iron/iron oxide RE (a) and the standard hydrogen electrode (SHE) scale (b), as a function of aqueous hydrogen concentration.

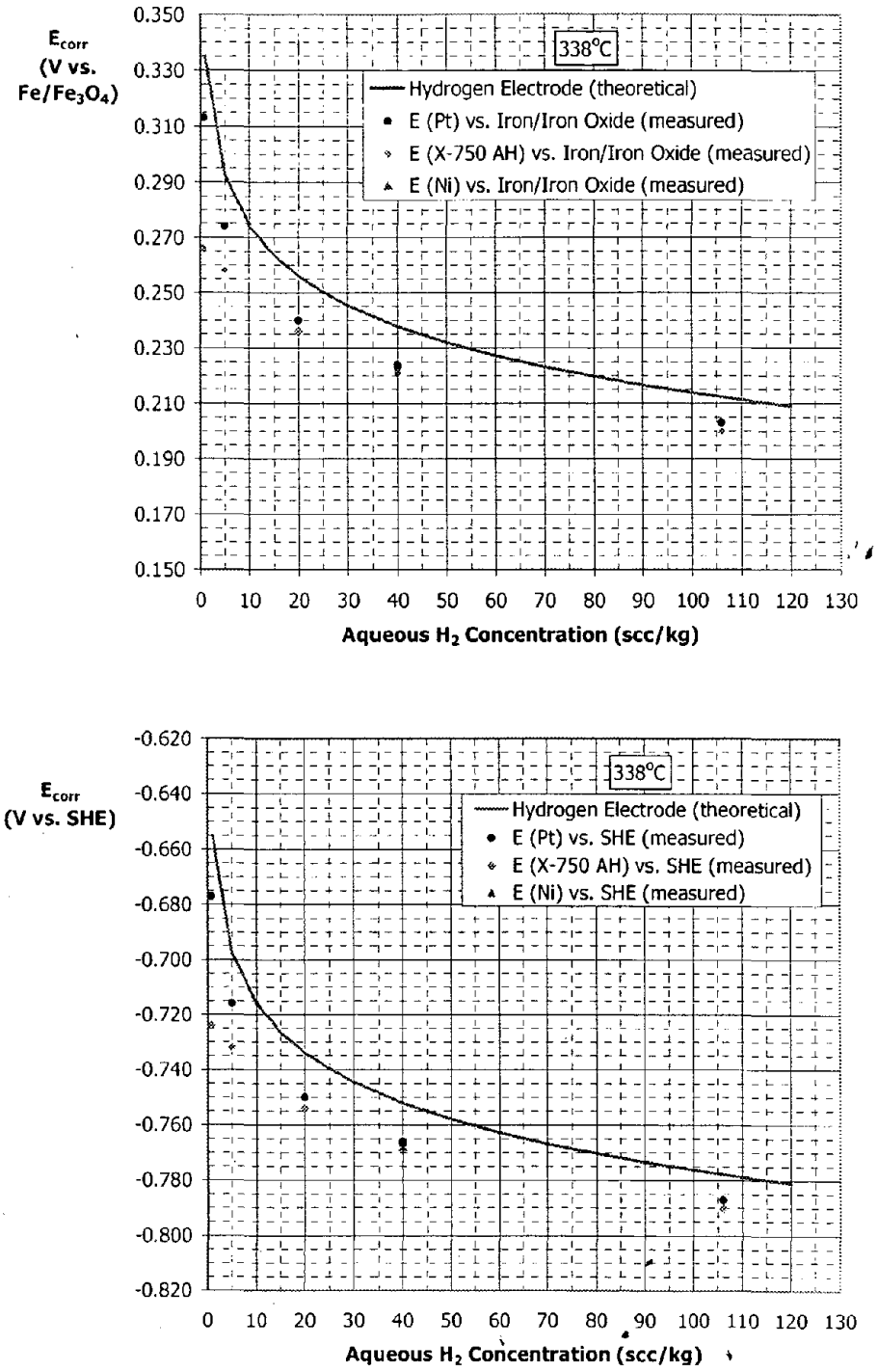

Figure 8. Electrochemical corrosion potentials (E_{corr}) at 338°C for platinum, nickel, and Alloy X-750 AH as well as the theoretical hydrogen electrode potential, *vs.* the iron/iron oxide RE (a) and the standard hydrogen electrode (SHE) scale (b), as a function of aqueous hydrogen concentration.

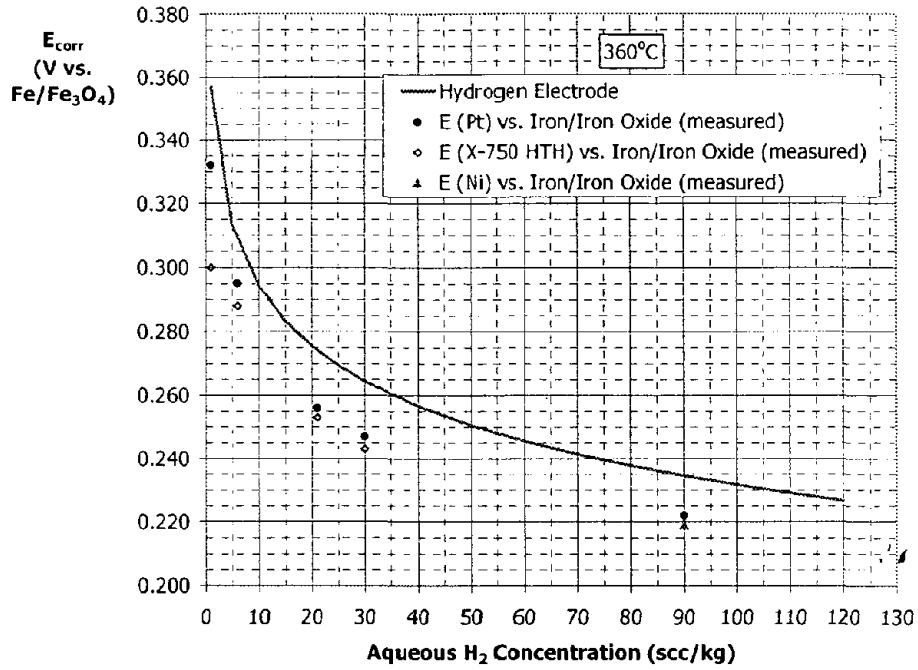

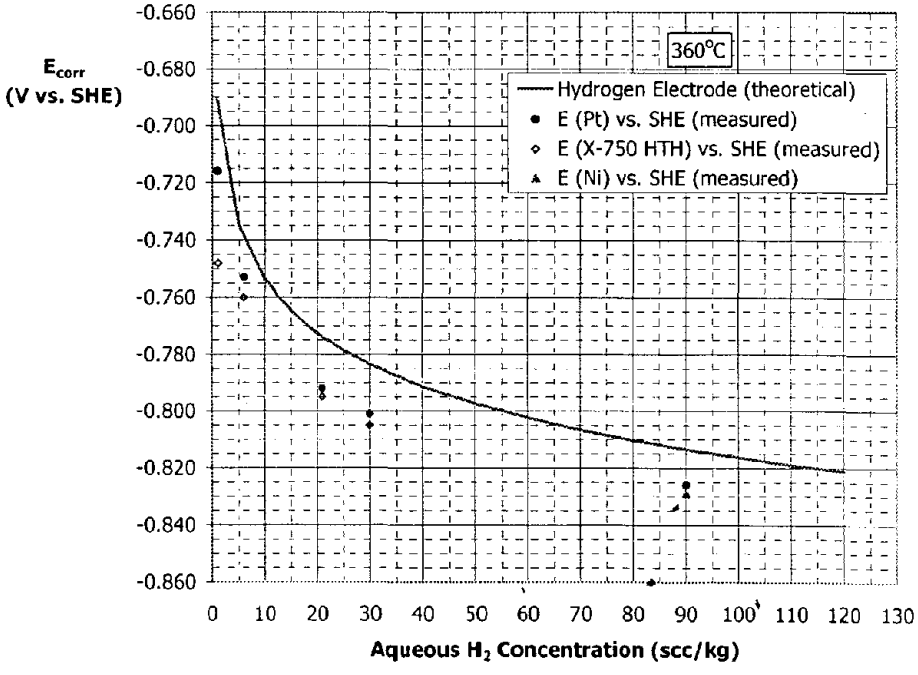

Figure 9. Electrochemical corrosion potentials (E_{corr}) at 360°C for platinum, nickel, and Alloy X-750 in the HTH heat treatment (X-750 HTH) as well as the theoretical hydrogen electrode potential, *vs.* the iron/iron oxide RE (a) and the standard hydrogen electrode (SHE) scale (b), as a function of aqueous hydrogen concentration.

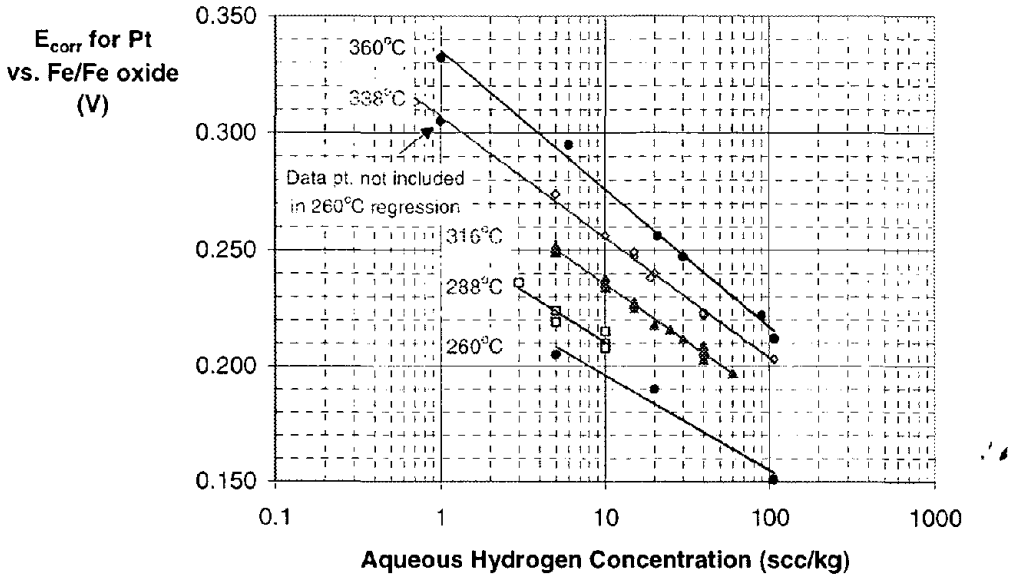

T (°C)	Measured Slope (V/decade)	Theoretical Slope (V/decade)	Percent Error	R^2
260	-0.041	-0.053	23	0.96
288	-0.044	-0.056	21	0.90
316	-0.050	-0.058	14	0.99
338	-0.052	-0.061	16	0.99
360	-0.059	-0.063	6	0.99

Figure 10. Semilogarithmic plot of the E_{corr} of Pt *vs.* Fe/Fe_3O_4 as a function of the logarithm of aqueous H_2 level at temperatures from 260 to 360°C. The data for each temperature are linear, as predicted by theory, and the measured slopes are in reasonable agreement with theory. One data point at 260°C is judged to be an outlier since it is the only data point out of 45 which is in clear disagreement with the other data points.

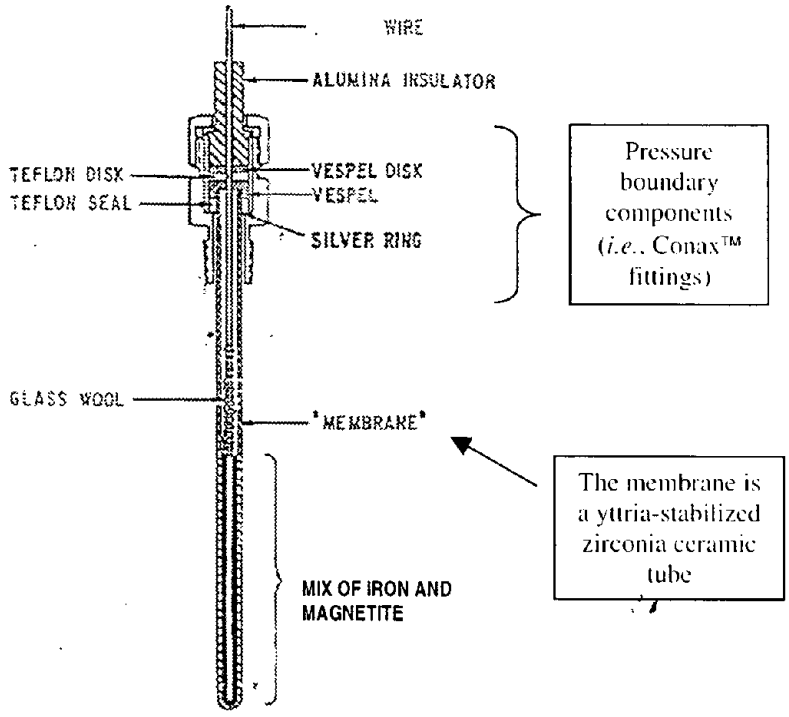

Figure 11. Schematic diagram of ceramic membrane reference electrode, taken from General Electric Corporate Research and Development Center [12].

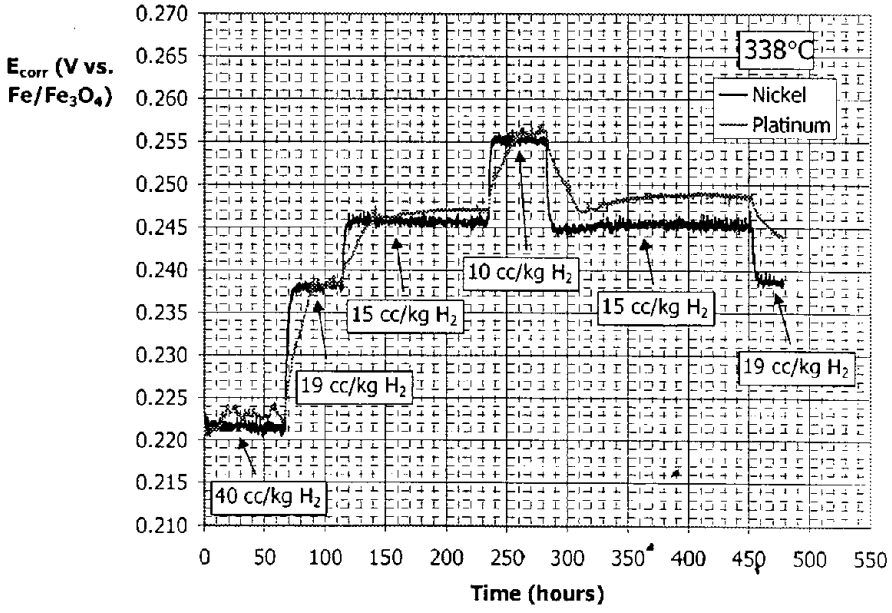

Figure 12. E_{corr} for Pt and Ni versus a YSZ/Fe-Fe_3O_4 electrode at 338°C, for different aqueous hydrogen levels. Note that the nickel specimen was consistently found to respond more rapidly than Pt to changes in aqueous hydrogen levels. This result was unexpected, as prior work on nickel-based alloys suggested that Pt response would be more rapid. This apparent difference between nickel and nickel-based alloys in terms of response time is not understood at present.

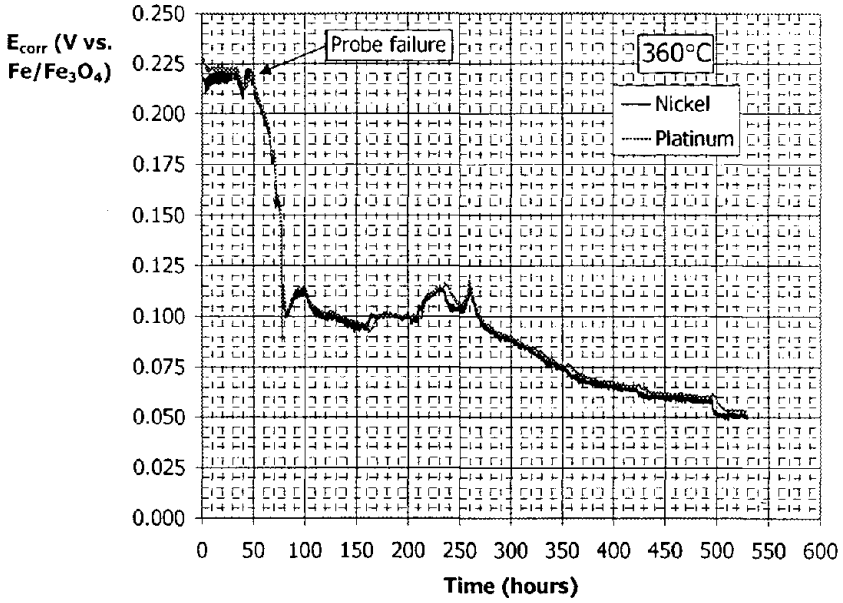

Figure 13. ECP versus time trace for a 360°C test which exhibited YSZ/iron-iron oxide reference electrode failure at approximately 40 to 60 hours into the test (note that the aqueous H_2 level was 90 cc/kg from 0 to 161 hours).

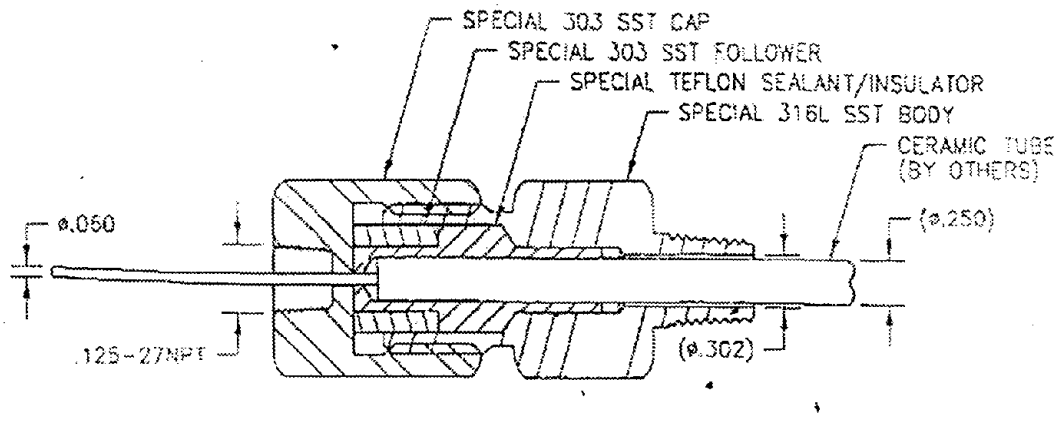

Figure 14. One of the new designs being used for the YSZ/iron-iron oxide reference electrode. This design employs a teflon sealant.

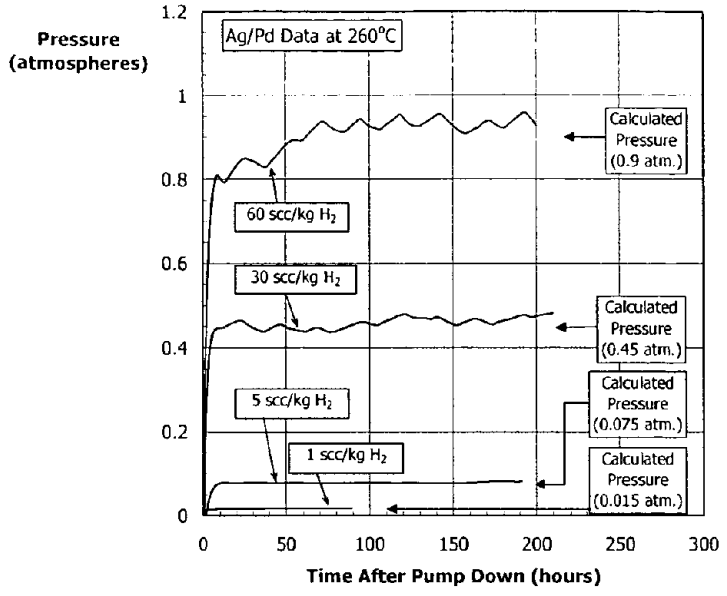

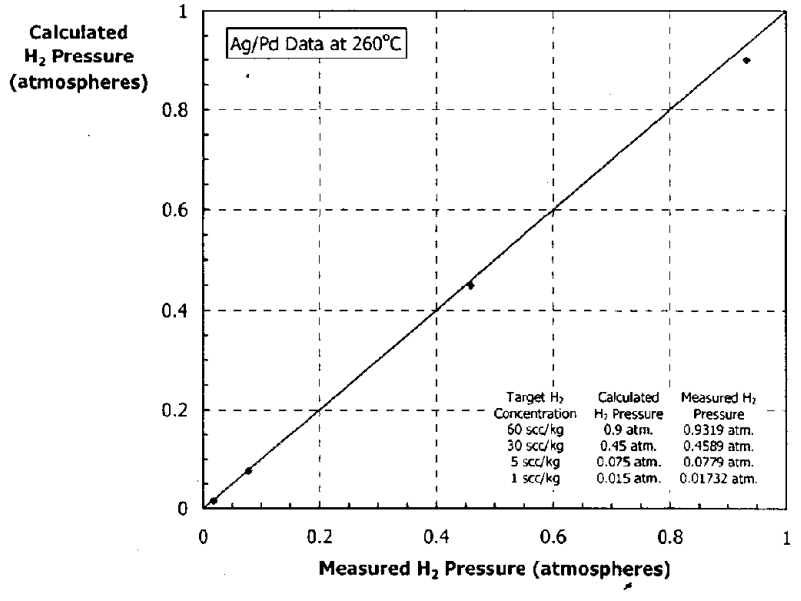

Figure 15. Hydrogen pressure measurements in a test autoclave at 260°C, conducted using a silver/palladium tube. Pressure transients are shown in (a) as a function of dissolved hydrogen concentration. In (b), the measured values are compared to values calculated using the Henry's Law coefficient in Table 1.

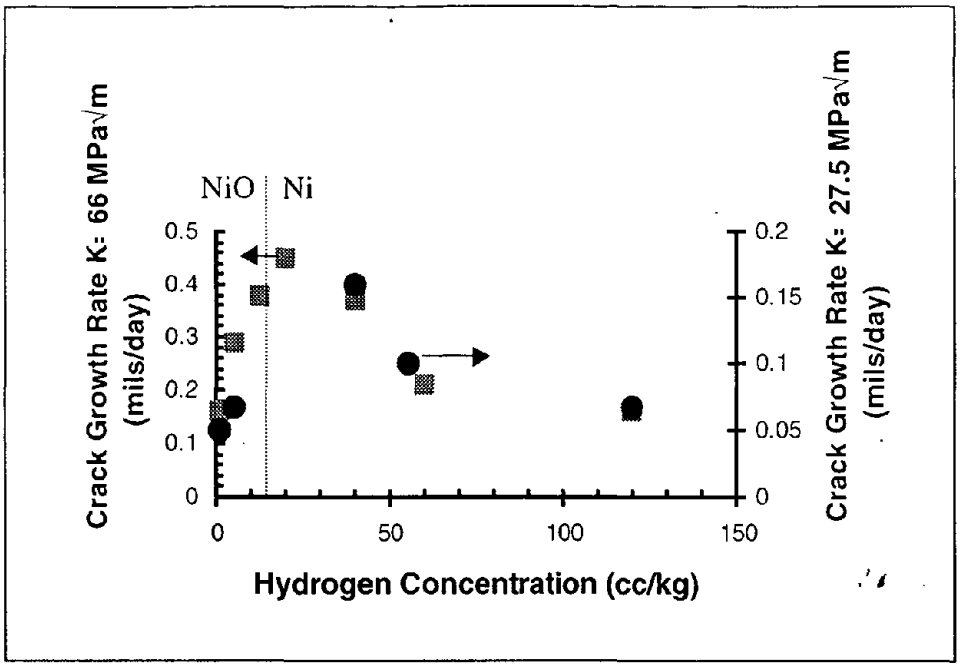

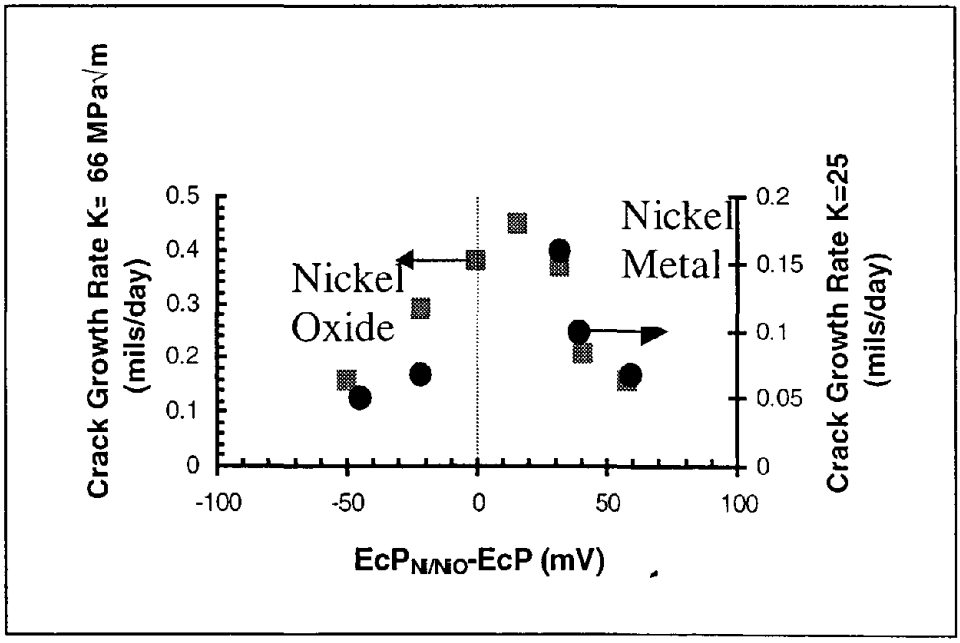

Figure 16. Alloy 600 crack growth rate at 338°C [8], plotted versus the aqueous hydrogen concentration (a) and the ECP difference versus the measured Ni/NiO transition (b). The Ni/NiO transition shown in (a) is based on CER and corrosion coupon data in [7], which indicate that the Ni/NiO transition at 338°C is located at 13.8 scc/kg H_2.

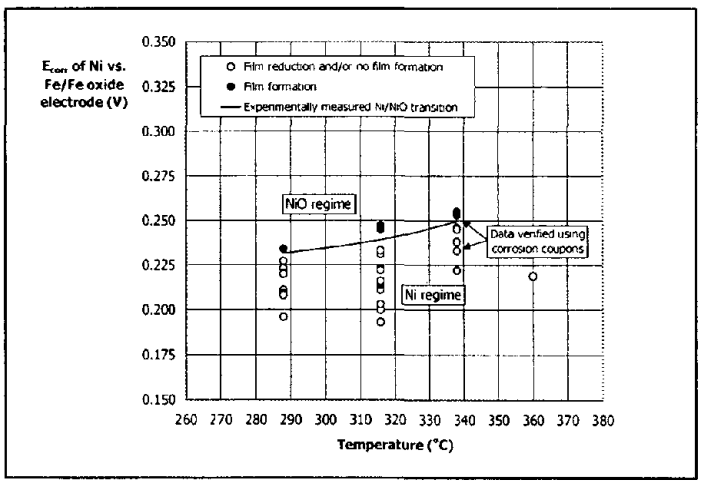

Figure 17. Ni/NiO phase transition measurements in ECP space [7]. This plot shows that ECP measurements *vs.* the YSZ/Fe-Fe_3O_4 RE can discern whether a given environment is located in the Ni or NiO stability regime.